

Quantum phase transitions in algebraic and collective models of nuclear structure

L. Fortunato,^{1,2}

¹Dipartimento di Fisica e Astronomia “G.Galilei”, Università di Padova,
v. Marzolo, 8, I-35131, Padova, Italy

²INFN, Sez. di Padova, v. Marzolo, 8, I-35131, Padova, Italy

July 29, 2021

Abstract

Quantum Phase Transitions arising in algebraic and collective models of nuclear structure are reviewed. The concepts of quantum phases and phase transitions are described as well as those of critical point symmetries and quasi-dynamical symmetries. Algebraic and collective models are compared and the connections between them are explored. Differences between even-even and odd-even systems are discussed. Several applications of critical point symmetries are given in both the even and odd sector. The spherical to γ -unstable and spherical to axially deformed quantum shape phase transition are covered in some detail as well as other transitions and alternative approaches.

Contents

1	Introduction	2
1.1	Previous review works on this topic	3
1.2	Note on previously assumed notions	4
2	What is a Quantum Phase Transition ?	4
2.1	Phases and Phase Transitions	4
2.2	Quantum Phase Transitions	5
2.2.1	History and names	5
3	QPT in nuclear physics	6
3.1	Types of mixing	6
4	Algebraic models	7
5	Collective models	8
6	Critical point symmetries	11
6.1	Quasi-dynamical symmetries	11
6.2	Critical point symmetries in even-even systems	12
6.3	Experimental evidence and searches for examples of the E(5) c.p. symmetry	15

6.4	X(5) critical point between spherical and axially deformed	16
6.5	Experimental evidence for examples of the X(5) c.p. symmetry	17
6.6	Y(5) and Z(5) c.p. symmetry	18
6.7	Other approaches to critical point symmetries	19
6.8	Critical point symmetries in odd-even systems	19
6.8.1	E(5/4)	19
6.8.2	E(5/12)	20
6.9	Experimental test of the E(5/4) symmetry in ^{135}Ba	20
6.10	Other candidates and the E(5/12) case	21
6.11	Comparison of even and odd cases	22
7	Algebraic models vs. collective models	23
7.1	Coherent states	24
8	QPT in even-even nuclear systems	25
8.1	Spherical to γ -unstable	25
8.2	Spherical to axially deformed	27
8.3	Density functional methods	27
8.4	Pairing-plus-quadrupole model	28
8.5	Approaches based on the SU(1,1) affine Lie algebra	29
8.6	Triaxiality	29
8.7	Pair-transfer	30
8.8	Mean-field PES mapped to IBM	33
9	QPT in odd-even nuclear systems	33
9.1	Spherical to γ -unstable in the odd case	34
9.2	Supersymmetry and quantum phase transitions	35
9.2.1	One-particle transfer	35
9.3	Spherical to deformed in the odd case	36
9.4	Prolate to oblate shape phase transitions in odd nuclei	36
9.5	Recent experimental and theoretical studies	37
10	Models with two-fluids	38
10.1	Two-fluids in algebraic models	38
10.2	Two-fluids in the BM collective model	40
11	Other models, other domains, other phenomena	41
11.1	Octupole	41
11.2	Excited state quantum phase transitions	42
11.3	Pairing phase transition	42
12	Conclusions	43

1 Introduction

Quantum Phase Transitions (QPT) represent a modern topic with a vast literature in more than a single domain of quantum sciences, therefore aiming at a complete description of all the ramifications is an arduous and unforgiving task, which goes beyond the reach of the present paper. Arduous because one should master several branches of physics down to their smallest details without losing sight of the

overall picture and unforgiving because, no matter the effort, something will escape even to the most meticulous worker and be noticed immediately by an attentive colleague.

Therefore, it is of the utmost urgency to clear the field right away from any misunderstandings and state that this review paper will cover introductory material and general topics as much as needed and then it will exclusively steer to the field of nuclear structure and, especially, to the description of quantum phase transitions occurring in algebraic and collective models of the nucleus. The selection of material has been approached from a theoretical angle and, in particular, the connections between algebraic models, symmetries, shapes and the transitions among them will be explored with a pedagogical attitude that, ideally, will stretch from the basics to the latest developments in the field.

This paper will initially give an overview of previously published material, then it will give a few definitions and discuss the special role that QPT in nuclei have gained through the years. The focus of the central part of the review will be on critical point symmetries and quantum phase transitions in even-even and odd-even system and a comparison thereof.

Alternative approaches and transitions in domains other than the quadrupole degree of freedom are also briefly discussed.

1.1 Previous review works on this topic

Let us mention that the study of quantum phase transitions in condensed matter physics is a field that has been growing at a fast pace, not only from the theoretical perspective, but also because experimental systems displaying quantum behaviour have become more and more experimentally accessible in recent years, from quantum dots to spin systems, from graphene to crystal lattices. Other topics such as superconductivity and Bose-Einstein condensation have many facets in common with nuclear structure and often the topics and the methodological approaches overlap. Sometimes instead, very similar systems are given a completely different treatment in these two branches of physics. From this richness, one cannot but hope for fruitful developments. Most of the material mentioned above is covered in the book edited by L.Carr [1] in which one of the chapters reserved for QPTs in domains different from condensed matter is Chapter 27, by F. Iachello and M.A. Caprio, where a systematic approach to QPT in algebraic models of nuclear structure is laid down. This is, of course, a precious *sine qua non* for the present review paper.

Another forerunner is the book by Sachdev [2], which starts from an introductory perspective and then delves into the complexity of the topic focusing on models (like the Ising model) and concepts (like scaling and universality) that are mostly found in condensed matter texts, but are somewhat marginal to nuclear theory. Often though, the mathematical approaches and the final aims are similar (or develop along parallel lines) and the reader might find it beneficial to compare them.

Among the books where various aspects of quantum phase transitions, and in particular of shape phase transitions, are explored, one should mention the book by R.F. Casten [3], where many subtle and crucial facts about the mixing of configurations and how to interpret them are explained in a simple and complete way, and the book of A. Frank, J. Jolie and P. Van Isacker [4], where several modern theories and ideas are collected. Another book where several chapters are related to the present paper is Ref. [5].

Another handful of papers [6, 7, 8, 9, 10, 11] are very useful to find more details on technical topics that are not covered here (excited state quantum phase transitions, connections with thermal phase transitions, non-quadrupole degrees of freedom, etc.) and to trace back the history of the field. The abundance of references testifies to the richness of this field. In Ref. [8], the initial sections deal with several simple experimental observables like the two-neutron separation energy or the ratio of energies $R_{4/2}$ between the first 4^+ and the first 2^+ , that show specific patterns such as discontinuities or flat behavior with respect to a change in the number of nucleons, thus indicating that some phenomenon is taking place.

In Ref. [11], the tables are very useful as they list several properties of bosonic models that display some QPT, in particular the order of the phase transitions and the relation to the cusp catastrophe.

1.2 Note on previously assumed notions

Throughout the paper it will often be necessary to explain abstract concepts that are most easily understood with some examples. Accepting the risk of breaking a strict logical ordering of topics, these examples are taken from the most common models and so I will assume that the reader has some smattering of fundamental models of nuclear physics such as the Bohr-Mottelson model or the interacting boson model. In other words, one should not expect to read in the following all of the basics facts about these two models from A to Z, or about basic notions of nuclear spectroscopy. Newcomers are referred to books such as those contained in the list of references, before starting to read the following.

2 What is a Quantum Phase Transition ?

To answer the question in the title of this section, one should define what a phase transition is and, to this end, one should clarify what a phase is in the first place.

2.1 Phases and Phase Transitions

Generically, a phase transition is a qualitative change in the physical properties of a system with respect to the variation of one or more parameters. The changing property is called the order parameter (n.b. it should be better called variable, rather than parameter), while the control parameter is the one that is made to vary by changing experimental conditions, or by sweeping some coefficient in a given calculation.

In classical physics, the word phase arises when one is dealing with different ways in which matter can occur, solid, liquid and gaseous that have clear morphological differences and respond to different physical laws, so that they appear as distinct domains, even though the chemical substance might still be the same (water for instance). Microscopically, it is linked to the concept of order and geometrical arrangement of atoms or molecules in different ways. Molecules are randomly oriented in gases, show a short-range arrangement in liquids and a long-range order in crystalline solids. Exceptions to this schematic divisions are not unusual and are part of the fun: for example, amorphous solids, do not show the long-range order mentioned above, but rather their molecules have a liquid-like arrangement, one might say that they are dense liquids with such a low mobility that they look solid at all practical effects.

The concept of correlations is also very important. These might be spatial short- or long-ranged correlations, as in non-magnetized ferromagnetic materials that locally show ordered structures known as Weiss domains or might be temporal, for example, certain liquids or solutions under the right conditions show a temporary order or a temporary polarization around charge centers. Any two clearly distinct phases often show a precise point, called the critical point, at which some sudden change happens and the switch between one phase and the other occurs as one crosses this critical point. The order of a phase transition is the degree of the derivative of some given quantity (either measured or calculated) that first displays a discontinuity. This way of classifying phase transitions is called the Ehrenfest classification [12].

Statistical or thermodynamic phase transitions, taking place in systems with a large number of particles ($N \rightarrow \infty$ is the so-called thermodynamic limit), usually show very sharp phase transitions, while transitions taking place in small systems with a finite number of particles, usually show less abrupt changes and less sharply defined transition points.

One might quantify the three regimes mentioned above with a range order correlator, i.e. a quantification of how a certain property of an extended system, described with either continuous or discrete variables, shows a degree of similitude over a certain spatial range. For example, for real scalar quantities,

$$\text{corr}(X, Y) = \frac{\text{cov}(X, Y)}{\sigma_X \sigma_Y}, \quad (1)$$

where σ is the standard deviation and $\text{cov}(X, Y) = \overline{(X - \bar{X})(Y - \bar{Y})}$ is the covariance. This is a familiar description in condensed matter, but seldom used in nuclear systems, therefore it will not be discussed in the following.

2.2 Quantum Phase Transitions

2.2.1 History and names

I have found it interesting to dig the literature and investigate the origin of the exact words “quantum phase transitions” in the context of nuclear physics. This has led me to find several misconceptions and omissions in the preceding works, that have often dismissed this topic inadequately, without delving into the references.

Usually, Robert Gilmore [13, 14] (together with Da Hsuan Feng, S.R. Deans and other coworkers) is credited for having introduced the concept of “ground-state quantum phase transitions” into current practice of the IBM [14]. In this 1981 paper, the symmetry triangle of the IBM is found to possess a line of first order phase transition, which is contained in a region of metastability between spinodal and antispinodal lines and ends on a second-order phase transition point on the vibrator to gamma-unstable edge of the triangle (U(5) to SO(6)). Despite being the first description of the phase transitions between the various symmetries of the IBM, the words “quantum phase transition” never appears in this paper.

One year earlier, in 1980, Dieperink, Scholten and Iachello in Ref. [15], using an algorithm due to Gilmore, Bowden and Narducci [16] and Gilmore and Feng [17], have found a way to associate a shape to the three dynamical symmetry of the IBM and have studied the phase transitions along the edges of the Casten triangle, finding a first order transition between U(5) and SU(3), a second order transition between U(5) and SO(6) and no phase transition between SO(6) and SU(3). In this paper the words “shape phase transitions” are used.

Curiously, in the letter preceding that of Dieperink, Scholten and Iachello, Ginocchio and Kirson [18] have introduced the coherent state appropriate for connecting the boson hamiltonian operators to shape variables, i.e., they have found a mapping from the IBM to the Bohr-Mottelson model, that proves very useful. This is a very important paper, but it does not mention the phase transitions though.

Although the concept was certainly invented and explored in the papers cited so far, the exact wording “quantum phase transition” appeared later in nuclear physics literatures and it was borrowed from condensed matter in a sort of mutual cross-fertilization.

Ref. [19] must also be mentioned because it recognized the importance of this concept very early, in the context of the Lipkin-Meshkov-Glick model, that is a 1D model for scalar bosons [20].

Let us also mention that the present paper is clearly dealing with zero-temperature, $T = 0$, phase transitions, as no thermal fluctuations are present or relevant in the realm of nuclei. The transitions are induced by a change in one of the control parameters in the hamiltonian of the system $H(\xi_1, \dots, \xi_n)$. There might be an exception in cases where the temperature is so high (here one deals with billions of degrees Kelvin, i.e., GK temperatures) that nuclear reactions and nuclear dissociation might take place: these are conditions that can barely be met at the center of massive stars or in exotic environments (for instance neutron stars, or in the plasma just a tiny bit after the big bang, etc.), therefore one can safely assume that all of these nuclear systems are far from showing thermal fluctuations.

3 QPT in nuclear physics

With the definition given above, quantum phase transitions in nuclear physics ultimately depend on the symmetry that is hidden in the model hamiltonian (or hamiltonians) that one is taking into consideration. So, despite all the wonders of nature, one is really dealing with the symmetry of a man-made model, rather than of true nuclei, although very often this is found to reproduce the observed experimental trends very closely. Typically, a model for QPT is designed in such a way to mix two limiting situations, and this is achieved through a number of ways, that are described in the following.

3.1 Types of mixing

Depending on the ingredients and the way in which they are cooked, the result might change. For example, for the sake of simplicity two different hamiltonians are made to mix *linearly*, i.e.,

$$\hat{H} = \xi \hat{H}_1 + (1 - \xi) \hat{H}_2 \quad \xi \in [0, 1] , \quad (2)$$

but there is no god-given rule that it must be so. One might invoke quadratic, or more involved ways to effect the mixing, such as a Fermi function or a logistic curve. For instance, without altering too much the previous expression,

$$\hat{H} = \xi^2 \hat{H}_1 + (1 - \xi^2) \hat{H}_2 \quad \xi \in [0, 1]$$

would change things (energy levels, wavefunctions and matrix elements) more smoothly in the region of small ξ 's and more abruptly close to 1. This is an often forgotten point: it is not only the hamiltonians you mix, but also the way you blend them, that affects the position of the critical point and how quickly one phase changes into another or coexists with another phase. One should properly refer to "linear" phase transition in the case of Eq. (2). For example, some of the differences that different parameterizations of $\xi(N)$ as a function of the number of bosons N induce on pair-transfer reactions treated within the IBM have been explored in Ref. [21].

Forgetting about the details of the parameterization, at an even more fundamental level, there are at least two ways in which two hamiltonians might be blended so to have a phase transition. The most obvious way is the admixing as in Eq. (2), but one might instead invoke a matrix mixing as in Ref. [22, 23, 24], where two different configurations are made to coexist:

$$\hat{H} = \begin{bmatrix} \hat{H}_a(\xi_a) & \hat{V}(\zeta) \\ \hat{V}(\zeta) & \hat{H}_b(\xi_b) \end{bmatrix} \quad (3)$$

where \hat{H}_a and \hat{H}_b are two hamiltonian operators for a single configuration that might undergo a phase transition depending on the control parameter ξ_a and ξ_b , respectively. The coupling operator \hat{V} controls the degree of mixing between the different configurations, depending on some other parameter ζ . Here ξ and ζ might also represent sets of parameters: for example if the hamiltonian is the consistent-Q hamiltonian (see Sect. 6.2) the set of parameters ξ might amount to two, the mixing between the monopole and the quadrupole parts and the χ parameter controlling the expression of the quadrupole operators. Ref. [25] refers to the situation expressed in Eq. (3) as intertwined quantum phase transitions (IQPTs), intending that shape changes and configuration-changes are intertwined. The parameter space of this alternative type of mixing is clearly more complicated. This type of mixing is also used in the special case in which a and b refer to a nucleus with configurations consisting in N and $N + 2$ bosons (i.e., with different core/valence spaces), thus including the possibility to study pair-correlations, pair-transfer phenomena and the like in systems where the requirement of particle number conservation is relaxed.

4 Algebraic models

Algebraic models allow to capture the essence of quantum phenomena and give a natural explanation of all the facts that depend on the symmetries of the problem. A certain quantum system is reduced to a number of degrees of freedom (d.o.f.) or basic blocks to which a certain angular momentum operator is assigned. These d.o.f. are scalars, vectors or tensors of higher rank (and might include pseudo-tensors as well) that represent either the relative motion between particles or, in turn, the spin or the total angular momentum of each of those particles. For example, in the Vibron model the p boson ($J = 1$) represents the vector distance between two atoms in a molecule. In the Interacting Boson Model, instead, the s and d bosons indicate the total angular momentum of a pair of nucleons coupled to $J = 0$ and $J = 2$ respectively.

The building blocks mentioned above, no matter their physical significance, are associated to a pair of creation/annihilation spherical tensor operators each, say b_m^\dagger and b_m , satisfying the usual commutation relations

$$[b_{m'}, b_m^\dagger] = \delta_{mm'} , \quad (4)$$

where the index refers to the third component of the angular momentum (that is unnecessary for scalar spin-zero operators).

After having chosen all the ingredients of a model, distinguished by capital letters $b(A), b(B), \dots$, one might list all the corresponding pairs of creation and annihilation operators and then form all possible number-conserving bilinear operators, i.e.:

$$\mathcal{G}_M^{(L)} = [b^\dagger(A)_m^{(j)} \times \tilde{b}(B)_{m'}^{(j')}]_M^{(L)} , \quad (5)$$

where the index in round parentheses indicates the rank of the tensors and the \times sign indicates the product between spherical tensors. The tilde sign is necessary to explicitly take into account the fact that the annihilation operators do not transform as spherical tensors. Thus, for bosons

$$\tilde{b}_m \equiv (-)^{m+k} b_{-m} , \quad (6)$$

where k is odd or even depending on the rank of b . The set of all the bilinear operators that can be formed in this way from the set of different b 's closes by commutation

$$[\mathcal{G}_i, \mathcal{G}_j] = \sum c_{ij}^k \mathcal{G}_k , \quad (7)$$

into a unitary Lie algebra that is taken as the spectrum generating algebra, g , for the model. Any hamiltonian built out of elements of the algebra and powers thereof can be diagonalized in a suitable basis, so one can say that the algebra $U(N)$ is a spectrum generating algebra for the particular model that has been chosen. Here N , the rank of the unitary algebra, counts the number of different operators that originate the algebra. For instance in the vibron model, the operators are $\{s, p_{-1}, p_0, p_1\}$ and the algebra is $U(4)$, while in the IBM the operators are $\{s, d_{-2}, d_{-1}, d_0, d_1, d_2\}$ and the algebra is $U(6)$. One might formulate the most general hamiltonian with the building blocks of an algebra as a scalar operator of the form:

$$H = E_0 + \sum_k \alpha_k \mathcal{G}_k + \sum_{kk'} \beta_{k,k'} \mathcal{G}_k \mathcal{G}_{k'} + \dots , \quad (8)$$

where E_0 is some constant parameter (that fixes the energy offset) and where \mathcal{G} has been defined before. This notation does not make apparent that each \mathcal{G} is a bilinear operator, one could as well indicate it with the index of the creation and annihilation operators used to construct it. Upon rearrangement of the various terms appearing in Eq. (8), this expression is naturally divided into one-body terms, two-body terms, and so on. Often these terms are re-scaled with the number of bosons (or with the number

of particles in general), otherwise the importance of quadratic, cubic and higher order terms would dominate in the large- N limit, while one wants them to be smaller or comparable with the low-rank terms.

Now the dimension of the unitary algebra that was already referred to is, in general, not small and there are a number of possible subalgebras of g and a number of possible subalgebra chains, that is to say concatenations of algebra/subalgebra relationships such as $g \supset g'_i \supset g''_i \cdots$ eventually ending in a one-dimensional algebra. Each concatenation gives rise to a possible choice for the basis states (see Chen [26] and Iachello [27] for a more detailed discussion of theorems and definitions, in particular, the problem of branching and missing labels). The structures representing the first layer (i.e. the first subalgebra in a given chain) are associated to “phases”, thus giving a precise definition of what is intended for phase in algebraic models: it is not only a symmetry, but it is one of the possible subsymmetries in a model of a well-defined symmetry. The mathematical procedure of obtaining all of these structures, called branching, is a difficult, but solved problem and it is amenable to algorithmic and computational investigations (see also [28]).

This leads us to the **definition of a phase in algebraic models of quantum systems** as formulated by Rowe [29]. Given a certain algebraic model, let g be its spectrum generating algebra and G the corresponding group. For any given chain of subgroups $G \supset G' \supset G'' \cdots$ of transformations of the physical system, the states of the system are said to be in a G -phase, when their properties are indistinguishable from those of the eigenstates labeled by the quantum numbers of the chain, belonging to the irreducible representations of that chain. This definition relies on an arbitrary criterion, i.e., that the properties are indistinguishable *up to a certain extent*, thus including not only the strict dynamical symmetry case (the limiting case where the the quantum numbers are valid), but also a larger region of the parameter space where the symmetry still holds, despite a small mixing with other phases. Iachello [30] gives a slightly simpler definition, identifying the phases with the dynamical symmetry of a certain model.

As an example, the familiar IBM, that is formulated in terms of an $U(6)$ symmetry, has only three dynamical symmetries, $U(5)$, $SO(6)$ and $SU(3)$, that can be associated with as many phases. These phases take names that are inspired by the collective model, spherical, γ -unstable and deformed, respectively, and are usually depicted with the help of the Casten’s triangle. In Fig. (1) one can see the extended Casten’s triangle, introduced in Ref. [31], where, together with three already mentioned phases, one can see also the $\overline{SU(3)}$ phase that correspond to a deformed oblate axial rotor, to be distinguished from the deformed prolate axial rotor, with symmetry $SU(3)$. This fourth symmetry appears in the consistent-Q formalism when one changes sign to the contribution of the d operators to the quadrupole operator.

In other algebraic models, there might be a proliferation of phases, with growing dimensions of the underlying unitary algebra $U(N + 1)$, but two special subalgebras are always present, the maximal unitary subalgebra $U(N)$, very often called spherical, because it corresponds to potential models possessing a minimum in zero for a certain appropriate variable and the maximal orthogonal subalgebra $SO(N + 1)$, that is often called “deformed” by extension also in contexts that have nothing to do with deformation variables. These two algebras are connected in a very general way [32]. For high rank algebras there are also other possibilities and there might be semidirect sums to complicate the task of classification even further. Some other examples, like symplectic $Sp(6, R)$, or unitary algebras like $U(15)$ and $U(16)$, are reviewed in Ref. [33].

5 Collective models

Even though the collective model of Bohr and Mottelson (BM), also called Geometric Collective Model (GCM), has been formulated some 20 years before the IBM, it will be discussed after it, because,

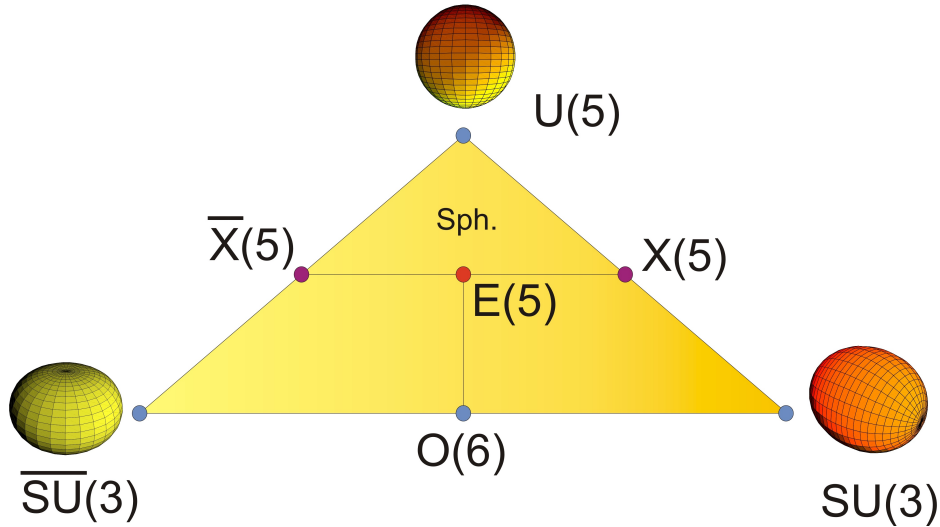


Figure 1: Extended Casten's triangle [31] showing the dynamical symmetries of the IBM and the critical point symmetries in between. Figure from Ref. [56].

referring in particular to the quadrupole degree of freedom, its dynamics can be “contained within” or “matched to” the algebraic structure arising from the IBM.

The BM collective model is the topic of innumerable textbooks, such as Ref. [34, 35] and reviews like [36, 37], to name just a few.

It treats the quantized oscillations and rotations of the nuclear surface by expanding it in spherical harmonics with a set of generalized coordinates $(\alpha_{\lambda,\mu})$. The familiar expression for the radius is

$$R(\theta, \phi) = R_0 \left(1 + \sum_{\lambda,\mu} \alpha_{\lambda,\mu} Y_{\lambda,\mu}(\theta, \phi) \right), \quad (9)$$

where R_0 is the radius of the spherical shape and the summation runs on $\lambda = 0, 1, 2, \dots$ and $\mu = -\lambda, -\lambda + 1, \dots, \lambda$. We are interested here only in the quadrupole degree of freedom ($\lambda = 2$) and the expression takes up a simplified form with only five parameters, $\alpha_{2,\mu}$, that describe all possible ellipsoidal shapes, spherical, axially deformed (prolate or oblate) and triaxial. After a rotation of the axes to the principal axes of inertia and another mathematical transformation to polar coordinates, the five-dimensional problem can be recast into a two-dimensional problem (having taken the Euler angles out of the game). The shapes mentioned above can be associated to a 60° wedge in this two-dimensional $\{\beta, \gamma\}$ plane, where $\beta^2 = \sum_{\mu} |\alpha_{\mu}|^2$ represents the extent of deformation and γ describes a deviation from axial symmetry. When $\gamma = \frac{\pi}{3}k$, with k positive, null or negative integer, two semi-axes are equal and the ellipsoid is either prolate or oblate. This is depicted in Fig. 2. When γ falls within the wedge the three semi-axes are unequal and the shape is triaxial.

These generalized coordinates can be used to set up a quantum hamiltonian in which a kinetic term is borne out of the momenta that are canonically conjugated to the α 's, namely by $[\alpha_i, \pi_j] = i\hbar\delta_{i,j}$ and takes up a quite complicated form (see Ref. [36] for details and further references) plus a potential representing a sort of restoring force acting on the nuclear shape. In brief, the Bohr hamiltonian can be written as

$$\hat{H}_B = \hat{T}_{vib} + \hat{T}_{rot} + \hat{V}. \quad (10)$$

where, dropping the operator notation, $V = V(\beta, \gamma)$ gives rise to different cases and interesting physics. The choice of Bohr and Mottelson, namely the harmonic oscillator in β with minimum in $\beta = 0$, gives rise to a spherical vibrator. The spectrum shows a typical harmonic pattern of degenerate energy states

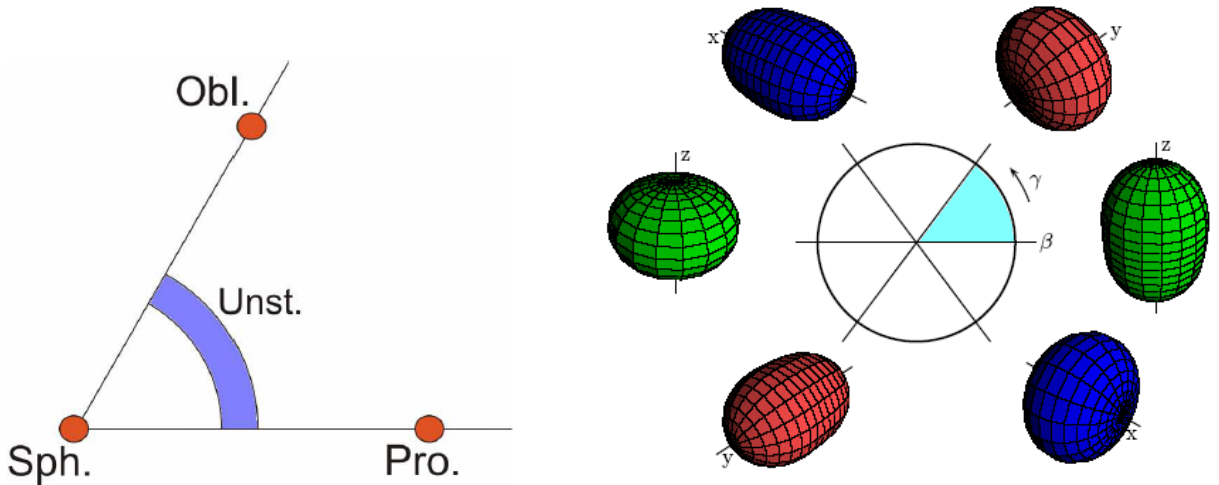


Figure 2: Left: Schematic representation of spherical, axial (prolate and oblate), and γ -unstable minima in the $0^\circ \leq \gamma \leq 60^\circ$ wedge. Right: Full $\{\beta, \gamma\}$ plane showing the symmetry axis and the Bohr relations across the six wedges.

due to the dimensionality of the underlying Hilbert space. It is quite a complicated problem of group theory to resolve all the branching relations and to count all of the degenerate states [38, 39, 40, 41].

More complex choices for the potential, generating localized minima on the sides of the 60° wedges give rise to axially deformed shapes, with typical rotational spectra with a $L(L+1)$ scheme that reminds of those of rigidly deformed molecules.

A third case is that of a potential that is independent of γ (like the harmonic oscillator case), but with a deformed minimum in β . One should picture it as a sort of circular trough in the $\{\beta, \gamma\}$ plane as in Fig. 2. This is the so-called γ -unstable solution of Wilets and Jean [42].

Depending on the position of the minima of a certain potential energy function, one speaks of shape-phases, associating each phase to a definite shape: spherical ($\beta_0 = 0$) or deformed ($\beta_0 \neq 0$). Amongst the latter, one speaks of prolate ($\gamma_0 = 0^\circ$) or oblate ($\gamma_0 = 60^\circ$) axial-rotors and finally of triaxial shapes ($0^\circ < \gamma_0 < 60^\circ$). These shapes can be put in correspondence with the limits of the IBM, through the formalism of coherent states (See Sect. 7.1).

A given potential yields well defined eigenspectrum and eigenfunctions, with certain typical features. most of which are collected in Refs. [36] and [43]. It is possible to construct families of models, i.e. potentials with parameters that bridge from a certain situation to another (for example from spherical to axially deformed) and study the variation of the energy spectrum and other properties along the phase transition. Examples of this are given in the following: Fig. 4 and corresponding text; Fig. 15 and corresponding text.

Using the BM model with potentials that parameterize a given phase transition can be very convenient as both exact analytical models and computer codes to solve the 5D Schrödinger equation are available.

While the IBM is extended to the odd-even counterpart (not without introducing complications), i.e. the IBFM, the extension of the BM collective model with the addition of an extra nucleon is not so straightforward and merges collective and single-particle aspects. Several attempts have been done in this directions, but treating the odd systems in the IBFM looks more promising, therefore this topic will not be covered here.

6 Critical point symmetries

A critical point symmetry is a dynamical symmetry that might show up at the critical point of a phase transition, depending on the functional form of the hamiltonian, although its occurrence is not ubiquitous. Some critical point symmetries, like E(5) for instance (see below), are symmetries showing up because some approximation has been taken or because some specific form of the potential has been chosen.

6.1 Quasi-dynamical symmetries

The common phase transition exemplified by Eq. (2) has been used in many cases, but it is illuminating to distinguish between two cases: one in which the two hamiltonians that are combined possess incompatible symmetries and one in which they possess compatible symmetries. The action of the two groups associated to each of the symmetries on the Hilbert space carrying reducible representations of both groups, are said to be incompatible if they do not commute with one another and there is no common subspace that is invariant under both groups. In a series of papers, Rowe and Rosensteel [29, 44, 45] discuss this issue in relation with the concept of quasi-dynamical symmetry¹. When two incompatible hamiltonians, i.e. two operators possessing symmetry properties connected with distinct Lie groups, are mixed, the typical outcome of a diagonalization is that it is possible to find a region, close to each symmetry limit, where the spectrum is relatively unperturbed and the states venture in the region of strong mixing without changing energy too much² *as if* they were still respecting the symmetries (degeneracies, energy ratios, etc.) of the exact limiting case, where the dynamical symmetry holds. This is called quasi-dynamical symmetry and it is illustrated in Fig. 3. In a narrow region around the critical point, that becomes narrower as $1/N$ as the number of constituents of the system, N , is increased, states do mix strongly connecting the two quasi-dynamical regions. The persistence of features that would normally be associated with the system having a certain dynamical symmetry, that can be seen in a number of experimental observables even in regions where mixing with another symmetry is taking place, is a somewhat intriguing fact. Mathematically, it can be traced back to the existence of embedded representations [29]. Suppose a system has a subset of states whose properties are in one-to-one correspondence with the properties (exactly calculated) of the irreps of a certain group, then one might say that those states span an embedded representation of G . As an example of this, the manifestations of the SU(3) symmetry in a subset of nuclear states have been recognized by Elliott well before this could be given a proper formulation inside a harmonic oscillator shell model theory, where the SU(3) symmetry is badly broken by the mixing induced by strong perturbation terms like the spin-orbit. In fact, ground-state rotational bands of heavy nuclei can be labeled very well with (λ, μ) quantum numbers and SU(3) enters in the definitions above of a quasi-dynamical symmetry.

The quasi-dynamical symmetry has also an important practical consequence. The dynamical symmetry is exact, but applies strictly only to the zero-measure extreme point of a phase transition (see discussion after definition in Sect. 4). Therefore, the chain of subgroups associated to it, can be used to label basis states that are strictly valid only at that point. The concept of quasi-dynamical symmetry extends the validity of the symmetry (and the validity of the basis) to a region of finite size, that runs almost to the critical point, becoming progressively larger and more reliable as N increases, where calculations can be carried out in the same basis, without too much mixing of configurations. This represents a computational advantage: one could diagonalize the problem in basis 1, arriving almost at

¹The widely used prefix “quasi” is borrowed from Latin and from this to the Italian language (and to English, French and German, at least). While in Italian it literally means “almost”, in Latin it rather had the meaning of “as if”. This translation makes the meaning of technical words such as quasi-spin, quasi-free quasi-elastic, much clearer to readers unfamiliar with Latin.

²Or, in absolute energy scale, without changing the ratios of their energies too much.

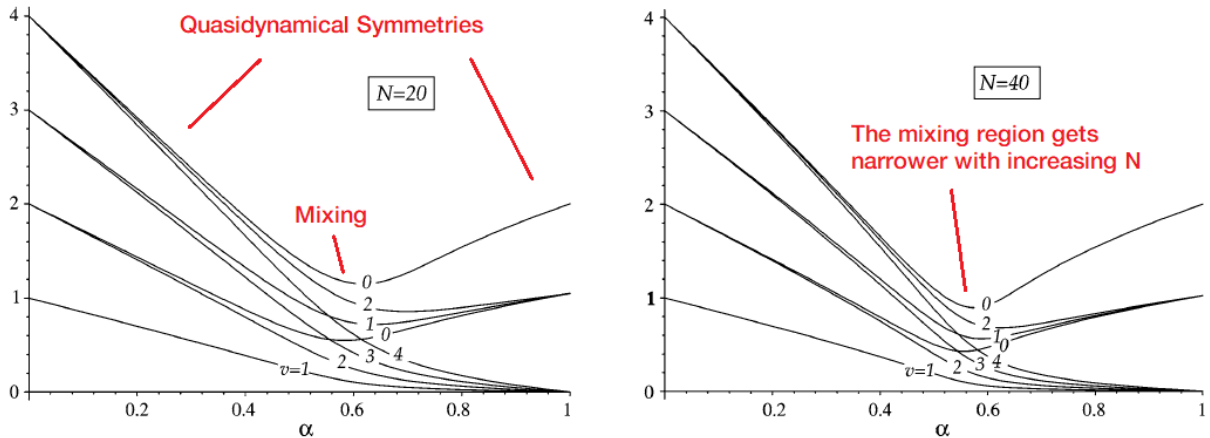


Figure 3: Energy spectrum of the linear mixing hamiltonian in Ref. [29] for $N = 20$ and $N = 40$ bosons. One can see the persistence of the energy ratios in the lateral regions where the quasidynamical symmetry holds. The regions where a strong mixing occurs, causing a reshuffling of the energy levels, gets narrower with increasing number of bosons. Taken and adapted from Ref. [29].

the critical point from one side and then diagonalize in basis 2, arriving at the critical point from the other side.

6.2 Critical point symmetries in even-even systems

Fig. 4 illustrates how the idea of critical point symmetry has arisen in the context of the Bohr-Mottelson model. The simplest potential, i.e., the 5D harmonic oscillator potential with parabolic behaviour in β and no dependence on γ , is the basis for the description of spherical nuclei. Considering that the simplest invariant operator of the model have a β^2 and $\beta^3 \cos 3\gamma$ dependence [34], and neglecting the γ -dependence for the moment, the first modification occurs as a β^4 term. If one stops at this level of complication, a quartic potential of the Landau-type can be written in the following form:

$$V(\beta) = a\beta^2 + b\beta^4 \quad \text{or} \quad \xi\beta^2 + (1 - \xi)\beta^4 \quad (11)$$

This potential bridges two cases: a spherical potential (pure $\sim \beta^2$) and a potential with a deformed minimum ($\beta_{min} \neq 0$). In between, a critical point, can be defined as the point at which the potential is purely quartic ($\sim \beta^4$), i.e., the point at which a deformed minimum appears and the origin is converted into a local maximum. This potential is flatter than parabolic close to the origin and steeper for large values of β . This potential, when inserted in the Bohr hamiltonian, does not admit an exact solution, but can be studied numerically with arbitrary precision [46]. However, as shown in the central panel of Fig. 4 one might approximate this potential with a square well [47], that, so to say, takes to the extremes the asymptotic behaviour at zero and infinity.

$$V(\beta) = \begin{cases} 0 & \beta < \beta_w \\ \infty & \beta \geq \beta_w \end{cases} \quad (12)$$

This γ -independent potential, that mimics the “true” one, admits an exact, parameter-free, solution with energies related to the zeroes of Bessel functions

$$\varepsilon_{\xi,\tau} = \left(\frac{x_{\xi,\tau}}{\beta_w} \right)^2, \quad (13)$$

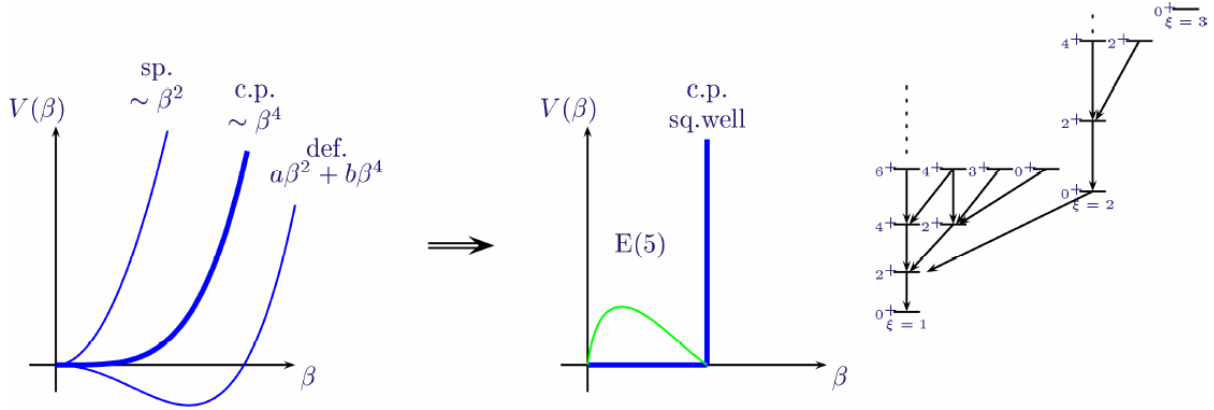


Figure 4: Left: γ -independent potential energy curves for spherical, critical point and deformed cases according to a Landau type potential; Middle: critical point square-well approximation for the potential at the c.p. and ground-state wavefunction; Right: E(5) spectrum. Adapted from Ref. [56].

where $x_{\xi,\tau}$ is the ξ th zero of the $J_{\tau+3/2}(z)$ function. The radial wavefunctions confined in the square potential well (green curve in the picture) are

$$f_{\xi,\tau}(\beta) = c_{\xi,\tau} \beta^{-3/2} J_{\tau+3/2}\left(\frac{x_{\xi,\tau}\beta}{\beta_w}\right) \quad (14)$$

and the normalization is found analytically from setting the integral $\int d\beta \beta^4 f^2(\beta)$ equal to unity. The γ -angular wavefunctions amount to the Bés functions [48].

The spectrum has a degeneracy pattern that is similar to other γ -unstable potentials, but has specific values for ratios of energies (normalized to the energy of the first excited 2^+) and ratios of other observables, such as electromagnetic transitions (normalized to the $2^+ \rightarrow 0^+$ transition). These ratios are close, but not identical, to the values given by the Landau-type potential at the critical point (the quartic potential). See also Ref. [49] for exact numerical results in the IBM with a very large boson number ($\simeq 10000$) that confirms that the critical point goes to the quartic behaviour in the classical limit.

This analytic exact solution has been called E(5) by Iachello, because the euclidean group in five dimensions arises in the algebraic formulation of this problem.

While E(5) is a beautiful conceptual scheme that sets a benchmark in low-energy nuclear structure, I believe that too much effort has been blindly devoted to search for nuclei that could match as close as possible with the predictions of the E(5) model, often forgetting that: i) it is an approximation, although a most remarkable one, of what is thought to be the true behaviour, i.e., quartic if one starts from the PES associated with a general IBM hamiltonian cut at the two-body level; ii) it was intended as a general interpretative scheme, a new mathematical paradigm to search for new physics and not as a strict set of rules to which the spectrum of nuclei must conform; iii) the whole Bohr-Mottelson model deals with the quantized motion of the nuclear surface, and while it gives a smart interpretation of the spectrum of most nuclei, it cannot be stretched far outside its inherent limitations (infinite number of particles, no evident connection to microscopic degrees of freedom, phenomenological inertial and stiffness parameters). Some of the limitations mentioned above can be resolved with more refined models or with a more accurate investigation. For example, the IBM elegantly connects the microscopic theory with the collective degrees of freedom and gives a way to go beyond the thermodynamic limit, allowing to do calculations with a finite number of particles (bosons in this case). Sometimes instead, these

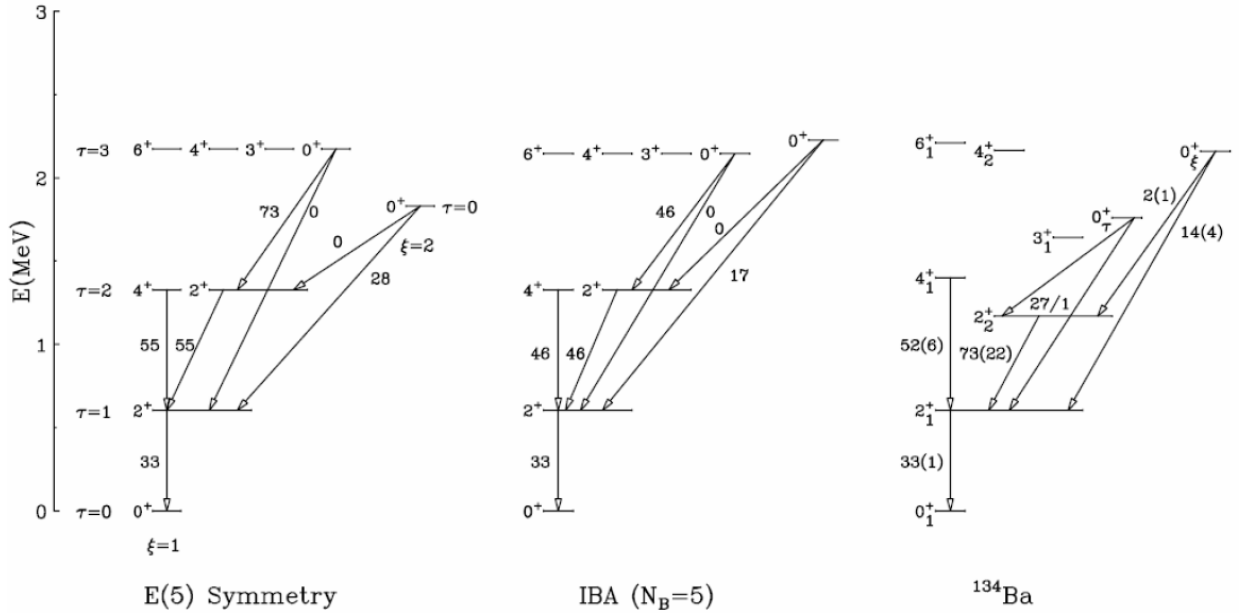


Figure 5: Comparison between the E(5) critical point symmetry, the IBM spectrum for $N_B = 5$ bosons and the experimental data for ^{134}Ba . States are labeled by the SO(5) quantum number τ , the family number ξ and by J^π . Arrows indicate B(E2) transition rates, normalized to the lowest. From Ref. [68].

limitations do not allow to match theory and experiments to a very fine grain. Many researchers have found smart ways to improve the predictions of theoretical models, but, in my opinion, too many uncertainties are still present at a coarse level, before one can really start adding parameters with the hope of a comprehensive description at a very fine level.

One can also see in Fig. 5, the comparison of the prediction of the E(5) model (as said, a special solution of the Collective Model with the γ -independent square-well potential) with an IBM (or IBA as it is also called, for Interacting Boson Approximation) spectrum for $N_B = 5$ bosons tuned to the case of ^{134}Ba , that is thought to be one of most important examples of a nucleus showing critical point behaviour. One can see that the effect of going from the analytic solution to the IBM calculation is not insignificant (notice the departure to high energy of the first excited 0^+ and the differences in electric quadrupole transitions) although it does not change dramatically the predictions. The comparison with the experimental data shows both good evidence and significant departure from such a remarkable description. Other effects, such as pairing, isospin, mixing with other type of internal excitations alter the attractively simple description given by the E(5) model. Much can be learned from an accurate analysis of the deviations, but, to my opinion, an excessive pursuit of absolute precision in fitting these states with a refined model, prevents the broader vision of the schemes that serve as a guide and form the backbone of forward-looking physical ideas.

The position of the critical points and of the critical line depend on the number of bosons. A simple calculation based on the consistent-Q hamiltonian allows to draw the critical line on the Casten's triangle as in Fig. 6. In this picture, that is the author's previously unpublished work, inspired by similar plots from Ref. [50], one can see the separation between the spherical and deformed phases, depending on the number of bosons, while in the mentioned reference, several other plots are drawn depending on the energy ratios.

The search for candidates of either the E(5) or the X(5) (next sections) symmetries has been done across the whole nuclear chart and it is still ongoing. The places to look for are somewhat in between

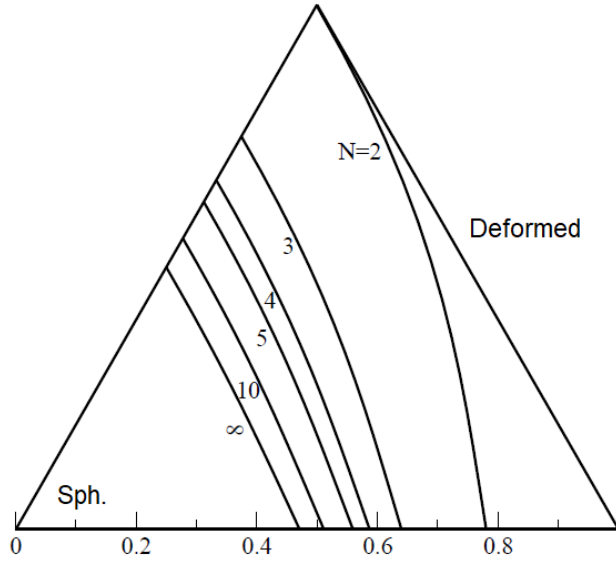


Figure 6: Critical lines drawn on the Casten’s triangle with varying number of bosons (the calculation indicated with ∞ has actually been done with $N_B = 1000$).

closed and open shells, as highlighted in Fig. 7. One expects a spherical regime (with energy ratio $E_{4^+}/E_{2^+} \sim 2$) for nuclei sitting near closed shells and a rotational regime ($E_{4^+}/E_{2^+} \sim 3.33$) for nuclei sitting at the center of open shells. Therefore, the prediction of the E(5) and X(5) schemes are to be searched in between. The isotopes that might fall close to the *loci* identified by these two symmetries are a handful for each shell and they have been thoroughly analyzed. For example, see Ref. [52, 53, 54, 51].

Electric quadrupole transition rates represent the most important observable aside from the more immediate energy ratios and energy level schemes, as they are the most direct probe of the wavefunctions. Sometimes models do predict energy levels that conform to actual data within certain limits, but they do not allow to distinguish. Quadrupole rates, that are more susceptible to the extension and overlap of wavefunctions, that in turn reflect the shape of the potentials that generate them, discriminate much more between seemingly equivalent options. Clearly, at the critical point, as well as for dynamical symmetry limits, most of these quantities can be calculated exactly, providing crucial benchmarks. B(E2) and quadrupole moments in the E(5) symmetry have been studied in detail by Arias [55]. Other quantities such as isotope shifts, transfer-cross sections, monopole transitions have been more sparsely used as a tool to address the problem of assigning a nucleus to a certain symmetry.

6.3 Experimental evidence and searches for examples of the E(5) c.p. symmetry

Several isotopes have been found that more or less closely match the predictions of the E(5) model [52]. It would be difficult to chose an optimal example, one should remember that the properties of nuclei depend on discrete integer numbers, N and Z , and the probability that one lands exactly on the critical point is very small, often one cannot but hope to be as close as possible. This, with the already mentioned approximations intervening when the potential is assumed as a square well, leads to the conclusion that, at most, real nuclei might loosely match these models. Again, I believe that a search for absolute precision is pointless, these are beautiful models, containing the physics and the germ of symmetry, but cannot be stretched out of their range of validity. The case of ^{134}Ba has already been discussed, in addition Jolos [57] describes various aspects of the second-order phase transition occurring

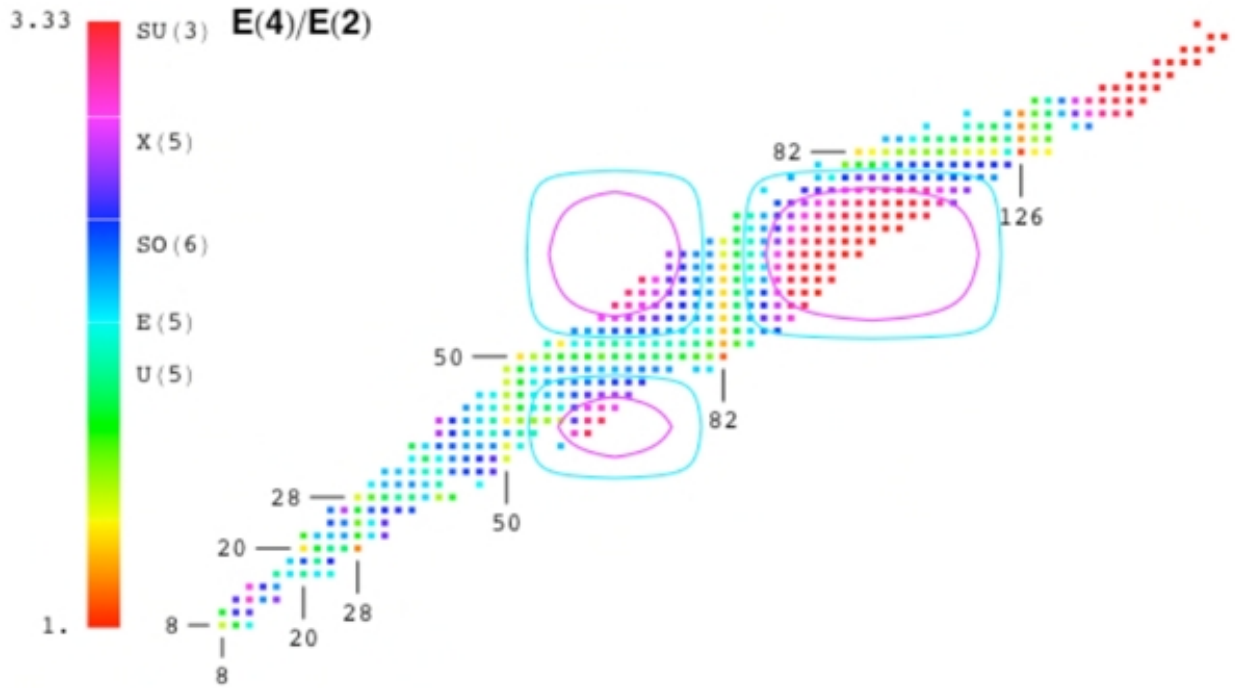


Figure 7: $R_{4+/2+}$ ratio across the nuclear chart (even-even isotopes only). Candidate regions for E(5) and X(5) nuclei are shown in blue and purple. From Ref. [56]. Courtesy of P. Van Isacker.

at the E(5) point, that is identified with a triple point, i.e., an isolated point at which phases change continuously, becoming indistinguishable, but without coexistence. Aside from ^{134}Ba that has been identified as the first candidate in Ref. [58], ^{102}Pd seems to offer good chances of being a candidate [59]. Other cases worth mentioning are ^{104}Ru [60] and ^{114}Cd [61], although it must be said that Cadmium isotopes are somewhat of a peculiar case, where maybe other phenomena must also be taken into account. Then, $^{128,130}\text{Xe}$ have been identified as possible candidates [52, 62, 63]. Xenon isotopes have also been investigated in Ref. [64], where a comparison of the IBM and the Bohr-Mottelson model with Davidson potential is made. See also Sect. 6.7 for a brief discussion of the case of ^{58}Cr .

6.4 X(5) critical point between spherical and axially deformed

Within the Bohr-Mottelson hamiltonian, the critical point of the first order quantum phase transition from spherical vibrator, U(5), to axially deformed rotor, SU(3), has been called X(5). This labels hints at some critical point in 5 dimensions, but it must be reminded that it does not represent a known algebra, hence the choice of the letter “X”. The same goes for other critical point “symmetries” that we will find in the following.

When one deals with this case the potential in the Bohr hamiltonian is a square well in β , exactly as in the E(5) case, but there is a minimum in γ around either $\gamma = 0^\circ$ for the prolate ellipsoid, or 60° for the oblate ellipsoid, see Fig. 2.

In Ref. [65], the Bohr hamiltonian has been treated with an approximated separation of variables, obtained by imposing

$$V(\beta, \gamma) \simeq V_1(\beta) + V_2(\gamma) \quad (15)$$

and by taking averaged values of $\langle \beta^2 \rangle$ in the γ -angular equation, that has the virtue of allowing for a simple formula for the energy spectrum and transition rates (see left panel of Fig. 8).

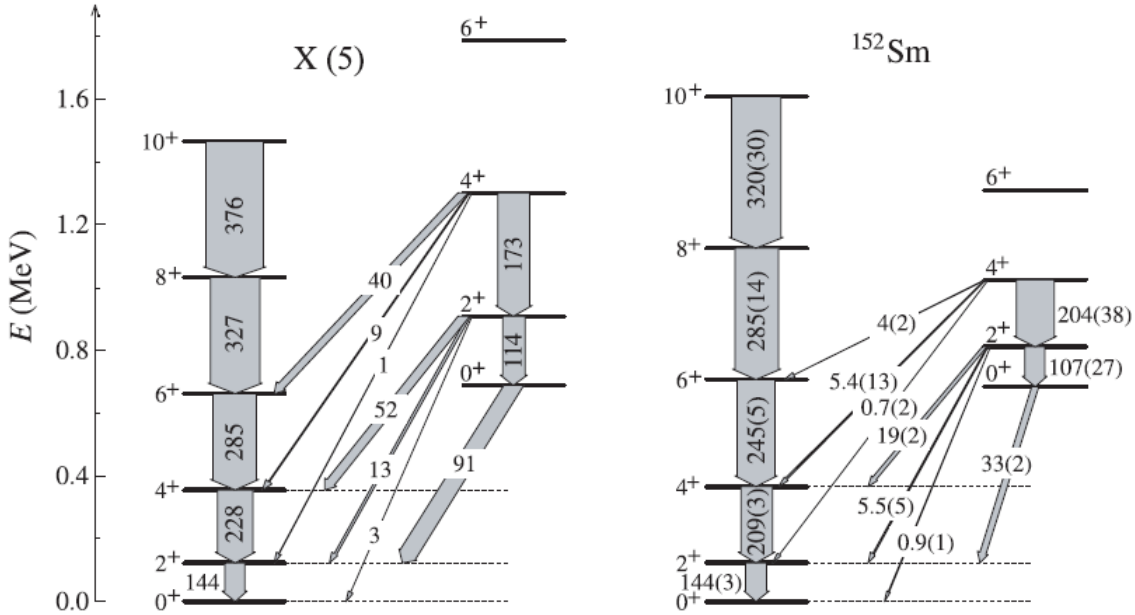


Figure 8: Comparison between the experimental spectrum of ^{152}Sm and the predictions of the X(5) model (with energies and transition rates normalized to the first excited state). Several B(E2) transitions are well reproduced by the X(5) model with some notable differences. Adapted from Ref. [7].

An exact numerical solution of the Bohr hamiltonian at the phase transition allows to assess the validity of the approximations and to establish the extent of the $\beta - \gamma$ couplings, that are found to be strong [66]. This was not apparent from the X(5) solution. The main difference is perhaps that the energy spacing of the β band is artificially enlarged by the presence of the rigid wall in the square well potential. The scheme of B(E2) transitions also shows several differences.

Despite being an approximation, that is not fully justified a priori, the X(5) solution works very effectively to describe the spectrum and other observables to a quantitative level.

The critical point symmetry between the U(5) and SU(3) can also be studied in the IBM, obtaining similar results but for a finite number of particles. A most important study on this topic, where comparisons are drawn and where other models like RPA are also used, is Ref. [45] (See Below Sect. 8.2).

6.5 Experimental evidence for examples of the X(5) c.p. symmetry

It has been suggested that several nuclei in the rare-earth region have spectroscopic properties that place them close to the predictions of the X(5) critical point symmetry (see for instance Ref. [6]). Most prominently, the N=90 isotones of Nd, Sm, Gd and Dy display spectra, transition rates and other properties such as two-particle transfer intensities [21, 67] that do show a significant agreement with the theoretical predictions. Initially, Casten and Zamfir [68] have found signs of the X(5) behaviour in ^{152}Sm . In Ref. [69], this isotope has been put to the test, identifying agreement of predictions and data for several observables, but evidencing also that there is at least one serious discrepancy of about two orders of magnitudes in the $2_{\gamma}^{+} \rightarrow 2_{2}^{+}$ B(E2) transition. This has been attributed to the separation of variables that is used in the X(5) model, while other models like IBM or the numerical solution of the

geometric collective model do not show this discrepancy. Bizzeti and Bizzeti-Sona [70] have proposed that also ^{104}Mo shows evidence of the X(5) symmetry. The energy spectrum is closer to the predictions than that of ^{152}Sm , for the ground, gamma, double-gamma bands and the first excited 0^+ state. Other possible candidates for X(5) can be identified [51] with the help of Fig. 7 (purple lines), although local considerations coming from the filling of shells (or the ordering thereof that might change far from the stability valley) might alter this simple picture. The isotope ^{154}Gd has been discussed in Ref. [71, 72].

A number of different empirical ways to quantify the extent to which a certain isotope need be classified into one of the various symmetries have been proposed. Limiting our discussion to the X(5), one could remember the work of Bonatsos et al. [73], proposing that the ratio of the first excited 6^+ and 0^+ states is effective in distinguishing between first- and second-order transitions that persists even in the large N limit. It turns out that the ratio $E(6_1^+)/E(0_2^+)$ behaves very differently in the rare earth region that is thought to exhibit a first-order shape phase transition, passing through X(5), than in the Ba-Xe region, that is believed to exhibit a second-order shape phase transition, passing through E(5). This ratio goes to 1 in the first case for large deformations and to 0 in the second case. This feature is proven to be independent of the boson number, thus providing a clear signature.

6.6 Y(5) and Z(5) c.p. symmetry

At least other two critical point symmetries, among others, have been discussed in the literature that deserve a mention: these are the Y(5) [74] and Z(5) [75] critical point symmetries. Only those in which no degree of freedom has been frozen (by invoking γ -rigidity for instance) will be briefly discussed in the present section.

Y(5) deals with the transition from axial to triaxial shapes [74] in terms of the angular variable γ . It uses a Landau type potential in the $\cos 3\gamma$ within the fundamental $0^\circ - 60^\circ$ wedge. Starting from the IBM-1, up to quadratic two-body terms, only constant and linear terms in this variable can be derived. One needs to go beyond the second-order and introduce three-body terms in the hamiltonian in order to be able to generate quadratic terms in $\cos 3\gamma$ in the coherent state approach. A potential of the type

$$V(\beta, \gamma) = f(\beta) - g(\beta) \cos 3\gamma + h(\beta) \cos^2 3\gamma \quad (16)$$

is obtained that can have either axial ($\gamma = k\pi/3$, with integer k) or non-axial minima, see Fig. 9 for an example of the latter category. This can be plugged into the Bohr hamiltonian with a suitable choice of the potentials in β and a second-order critical point, that is called Y(5), can be thus obtained. This symmetry has not been studied as much as the previous two symmetries, and examples have not been found in great abundance.

Z(5) instead has to do with the transition from prolate to oblate shapes. It is a parameter-free solution, obtained with an approximate separation of variables in the Bohr hamiltonian at $\gamma = 30^\circ$, with a square well in β . Some platinum isotopes are found to exhibit spectra that are in good agreement with the predictions of Z(5) [75].

The X(5) and Z(5) solutions have been generalized in the T(5) solution by Zhang and collaborators [76] that gives a scheme for the spectrum of the critical point transition from spherical to any triaxial with any $0^\circ \leq \gamma \leq 30^\circ$ (the rest of the wedge is obtained by symmetry around the central value $\gamma = 30^\circ$). The potential is again the sum of a square well in β supplemented by a shifted harmonic oscillator in γ around some equilibrium value, namely:

$$V(\gamma) = \frac{1}{2}C(\gamma - \gamma_e)^2 \quad (17)$$

which is very similar to what has been done previously for treating solutions around $\gamma_e = 30^\circ$ [77]. The same approximate separation of variables is used and then X(5) and Z(5) are naturally obtained at the limiting values of γ . The isotopes ^{148}Ce , ^{160}Yb , $^{192,194}\text{Pt}$ are analyzed in the same work [76], showing overall good agreement if γ_e is assigned the values 13° , 19° , 26° , 28° respectively.

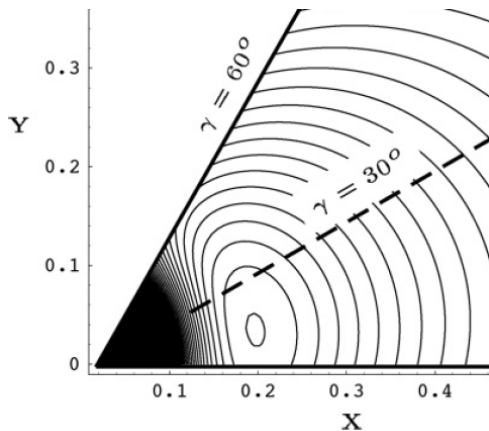


Figure 9: Schematic picture of a triaxial (non-axial) minimum of the potential energy surface in the β, γ plane. Excerpt from Ref. [77]. The cartesian coordinates are related to the polar deformation coordinates by $X = \beta \cos \gamma$ and $Y = \beta \sin \gamma$.

6.7 Other approaches to critical point symmetries

The Relativistic mean field (RMF) theory has also been applied to the case of phase transitions by solving a generalized version of the single-particle Hartree-Fock-Bogoliubov hamiltonian in which nucleons are treated covariantly and the interactions are mediated by the exchange of virtual mesons, using the NL3 force [78]. It was possible to produce Potential Energy Surfaces (PES) that showed rather flat behaviour in the internal region of the potential, thus justifying the assumption of the E(5) symmetry. The corresponding cases for the X(5) symmetry show a bump in the potential that justifies the first order character of this phase transition.

An analysis of the E(5) shape phase transitions in the even-even $^{52-66}\text{Cr}$ isotopes has been conducted with the constrained relativistic mean field theory [79] using various effective interactions. The PES indicates the ^{58}Cr isotope might be a good candidate for E(5) symmetry, showing independence on γ and a flat behaviour in β . This opens up a new region of relatively low mass isotopes for further investigation.

6.8 Critical point symmetries in odd-even systems

6.8.1 E(5/4)

When trying to extend the concept at the basis of the E(5) symmetry to odd systems, one faces the question of where to place the additional particle. There is some mixed jargon here and in the following, because while the bosonic core can be treated either in the CM or in IBM, the extra nucleon, i.e. the fermionic degree of freedom, is treated as a single-particle in mean-field models. Once again symmetry is the unifying factor, whatever the model is, it can be recast into a Lie algebra language and thus the identification of bosonic-fermionic symmetries or supersymmetries makes the unification easier.

The first case identified by Iachello consists in placing the fermion on a $j = 3/2$ orbital, therefore giving rise to a boson-fermion symmetry in which the bosonic part is U(5) and the fermionic part amounts to the unitary algebra U(4). The symmetry at the critical point has been called E(5/4) [80]. This is a particularly relevant case, because it is known from the work of Bayman-Silverberg [81] that the symmetry of the $j = 3/2$ fermionic orbital, when coupled to the Bohr-Mottelson collective model, gives rise to supersymmetry, identified with the U(5/4) Lie superalgebra. This preserves the γ -instability and possesses a number of peculiar features such as a degeneracy of multiplets, but clearly limits the

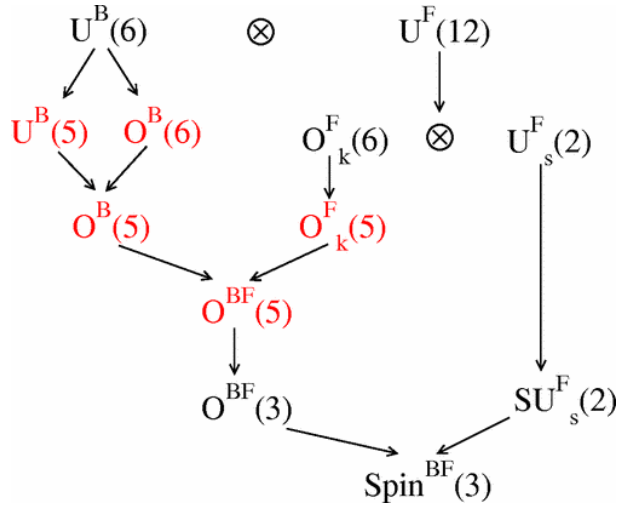


Figure 10: Lattice of subalgebras of the $U(6/12)$ model that passes through the $O^{BF}(5)$ algebra, that is common throughout the whole transition from spherical to γ -unstable. Courtesy of A. Vitturi.

occurrence of this symmetry to cases where a single nucleon occupies a p or d orbit (see Sect. 6.9). Several properties of nuclei at the transitional point are worked out in Ref. [82]. Clearly, this is an attractive approach, but forgets about the complex microscopical nature of the core nucleus. It is, in fact, difficult to conceive that odd medium- or heavy-mass nuclei might show a perfect separation of this single-particle orbital relatively far from closed-shells, without any sort of particle-hole excitations coming into the way. Therefore, the degree of applicability of the critical point symmetries to odd nuclei is a bit more impaired than in the even-even sector.

6.8.2 $E(5/12)$

Another important case occurs when the fermion is free to roam in a multiplet of single-particle states with $j = \{1/2, 3/2, 5/2\}$ [83]. This might happen around $A=190$ mass region, thus opening up the possibility to observe this symmetry in Pt or Ir for example. In this case the fermionic algebra is $U_F(12)$ and the corresponding analytic solution is called $E(5/12)$. This critical point superalgebra can be compared with the quite complex lattice of subalgebras that comes from the coupling of bosonic and fermionic algebras of the IBFM, see Fig. 10.

The $U_F(12)$ can be thought as arising from a pseudo-spin and a pseudo-angular momentum (either 0 or 2), where the latter transforms as the (0,0) and (1,0) representations of the $O_F(5)$ subgroup. This suggests a simple boson-fermion coupling scheme based on an extension of the quadrupole operator to the boson-fermion sector. The ensuing model is analytically solvable and gives results that are comparable to those obtained by the IBFM at the critical point, as in Fig. 11. Here states are labeled by the set of quantum numbers $\{\xi, \tau_1^B, \tau_1^F, (\tau_1, \tau_2)\}$ where ξ labels families of states similarly to the $E(5)$ symmetry and the various τ correspond to the quantum numbers appearing in the eigenvalues of the invariant operators for the five dimensional orthogonal groups appearing in the lattice of Fig. 10, labeled with B, F and BF (two quantum numbers).

6.9 Experimental test of the $E(5/4)$ symmetry in ^{135}Ba

The work of Fetea et al. [84] is the first experimental verification of the extension of the concept of critical point symmetry to the odd-even case. In particular, they have analyzed the case of ^{135}Ba as

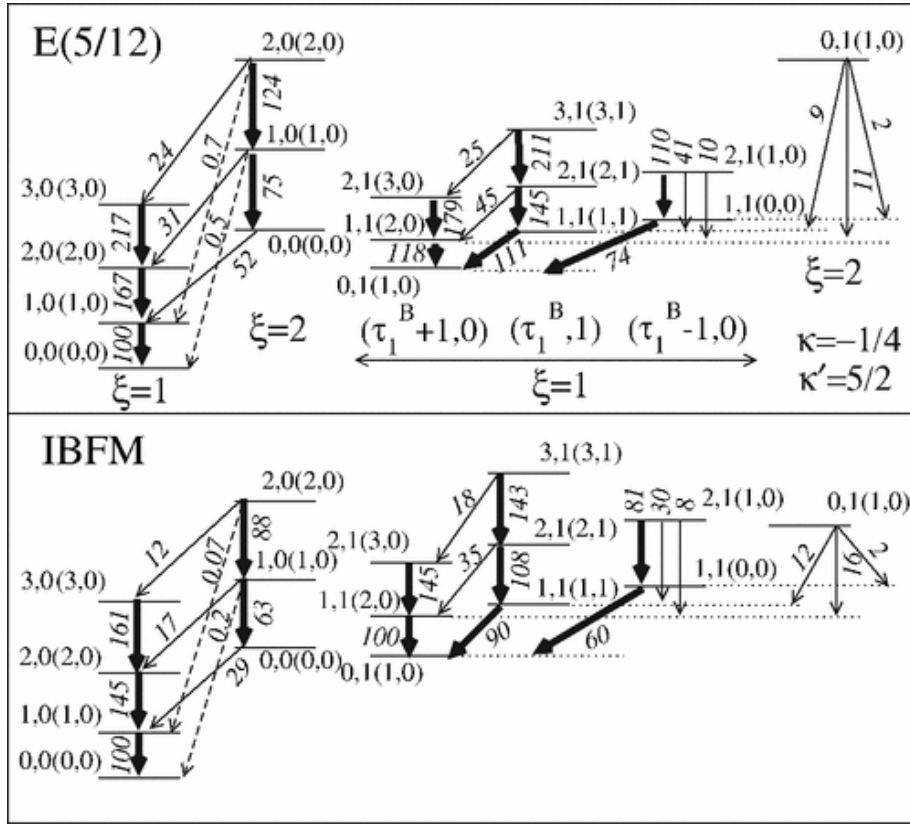


Figure 11: Comparison between the spectrum of the E(5/12) model, in which states are labeled by the $\xi, \tau_1^B, \tau_1^F, (\tau_1, \tau_2)$ quantum numbers and the spectrum at the critical point of an IBFM hamiltonian. See Ref. [83] for further details such as the values of parameters and explanation of labels and BE(2)'s. Notice that each multiplet in parentheses correspond to a set of angular momentum values. Courtesy of A. Vitturi.

an extension of the E(5) case of ^{134}Ba plus a neutron occupying a $j = 3/2$ orbital. This should be an optimal test-case for the manifestation of the E(5/4) symmetry. The β -decay experiment showed agreement in several observables as well as significant disagreement. The first obvious consideration, from shell model perspective, is that the neutron is probably not fully in the $2d_{3/2}$ orbital, but roams in a larger model space and a second consideration is that a number of low-energy particle-hole excitations are going to affect the spectrum, therefore one cannot expect that the spectroscopy of this isotope would perfectly adhere to the predictions of the collective model. Indeed, it is not surprising that the degeneracy of the multiplets is broken even more than it would be for even-even cases. Both the IBFM and the shell model predictions better agree with data, at the price of additional parameters. It is, in fact, more difficult to save the simplicity of the critical point symmetries in the case of odd-even nuclei.

6.10 Other candidates and the E(5/12) case

Other candidates as examples of the critical point symmetries in odd nuclei are ^{129}Xe (by Harissopoulos, see discussion in Ref. [85]), the Ir-Au region, where the U(6/4) supersymmetry shows up, and ^{63}Cu . Jolie *et al.*[86] discussed the possibility that osmium-mercury region might give good examples of the U(6/12) supersymmetry and shape phase transitions in the IBFM with single particle orbits $j = 1/2, 3/2, 5/2$.

The paper [87] discusses in detail the theory of supersymmetry in nuclei and it reports several experimental observables and where and how the supersymmetric scheme matches with experimental

data in various regions of the nuclear chart.

6.11 Comparison of even and odd cases

The even-even and odd-even systems differ just by a single nucleon, but this is not a simple $1/A$ effect as one might imagine at a first guess. The addition of a fermion changes the properties of the system and the underlying symmetries much more than it could be naively expected. At low energies the core behaves as a boson condensate in which the building blocks are bosonized and the addition of just one more spin-1/2 particle alters the state of affairs. Even without evoking exchange properties with the fermions hidden inside the condensate (either core or valence bosons), first of all the symmetry chains and the set of quantum numbers are completely different. An approach entirely based on a full fermionic model (if feasible) would miss the role of the boson condensate, that drives the change in structure along the transitional path.

Fig. 12 shows a comparison of energy levels of the even-even system and the odd-even system (with the fermion sitting in a $j = 3/2$ state) performing a phase transition described with the IBM hamiltonian

$$H = H_B + H_F + V_{BF} \quad (18)$$

that is the sum of a bosonic, a fermionic and a boson-fermion interaction and allows to move from the spherical to the gamma-unstable limits by changing the parameter $x \in [0, 1]$ that appears in a consistent-Q hamiltonian for the even-even part

$$H_B = x\hat{n}_d - \frac{(1-x)}{N}\hat{Q}_B \cdot \hat{Q}_B \quad (19)$$

and in the coupling between the respective quadrupole operators

$$V_{BF} = -2\frac{(1-x)}{N}\hat{Q}_B \cdot \hat{q}_F. \quad (20)$$

The critical point is marked by the dashed-dotted line in both panels. Energies are normalized to the energy of the first state or to the energy of the first degenerate multiplet in the odd case. All states or multiplets are labeled with the total angular momentum (that is integer or half-integer respectively) and, in round parentheses, with the SO(5) quantum number τ and with the pair of Spin(5) quantum numbers, called (τ_1, τ_2) , appearing also in the preceding section. Note that there is no parity quantum number on the states of the odd system, as this depends on the parity of the fermionic orbital, which is left unspecified. The overall behaviour is quite similar, except that the odd system has a larger number of states and it has a larger number of branchings. Take for example, the first excited multiplet: it is divided into a $(3/2, 1/2)$ and a $(1/2, 1/2)$ multiplets quite soon, even before the critical point. The same, to an even larger degree, happens for higher lying multiplets. The odd system is further labeled by the σ_1 asymptotic quantum number, which is strictly valid only in the limit $x = 0$.

The importance of having chosen the $j = 3/2$ orbital, giving rise to a quite unique supersymmetric case, is highlighted in Fig. 13 where a comparison of spectra is drawn. The one on the left is the same as in Fig. 12, but absolute energies are displayed, while that on the right depicts the spectrum of a $j = 5/2$ fermionic orbital coupled to the same bosonic core (here $N_B = 7$ is taken as a reasonable number, but the actual value is, of course, irrelevant to the present discussion). The degeneracy is broken in the second case, and each state of the multiplet follows its own pattern, although their shape is quite similar. These are now absolute energies, rather than normalized as in Fig. 12, exactly because the comparison would be impaired by the removal of degeneracy in the second case. Notice that the order in which the first multiplet splits would not be easy to guess, $7/2, 1/2, 9/2, 3/2$ and $5/2$ from low to high.

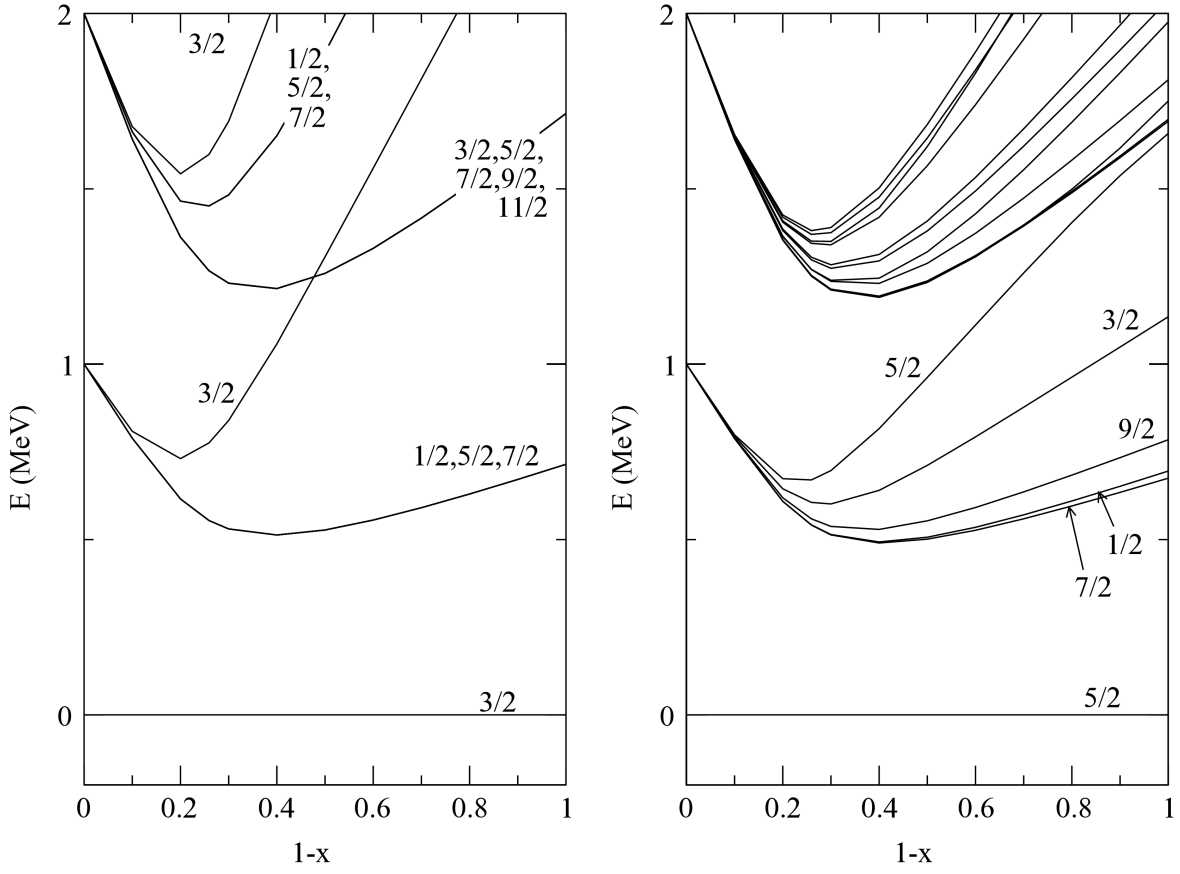


Figure 13: Energy levels of the odd system displayed as a function of the parameter x considering the odd particle in the $j = 3/2$ orbital (left panel), supersymmetric case, and in the $j = 5/2$ orbital (right panel) for the sake of comparison. The number of bosons is $N_B = 7$ in both cases, though the actual number is immaterial. The point here is that the $j = 3/2$ orbital does not break the $U(6/4)$ symmetry and the multiplets show a typical degeneracy pattern, that is lifted in the picture on the right.

7.1 Coherent states

The technique of intrinsic or coherent states³ can be used to connect any bosonic hamiltonian, like those of the IBM, with an energy surface and a Bohr hamiltonian in terms of quadrupole shape variables [93].

The normalized boson condensate is given by the coherent states [13, 15, 17, 94]:

$$|g; N, \beta, \gamma\rangle = \frac{1}{\sqrt{N!}} (\Gamma_g^\dagger)^N |0\rangle \quad (21)$$

with

$$\Gamma_g^\dagger = \frac{1}{\sqrt{1+\beta^2}} \left[s^\dagger + \beta \cos \gamma d_0^\dagger + \frac{1}{\sqrt{2}} \beta \sin \gamma (d_2^\dagger + d_{-2}^\dagger) \right] \quad (22)$$

being the basic quadrupole boson creation operator. It is constructed with the scalar and quadrupole operators of the IBM-1. The energy surface, for a given IBM hamiltonian \hat{H} , is given by the expectation

³Introduced originally by Perelomov [92] as a mathematical technique that allows to connect the unitary irreducible representations of a compact group with an orthonormal basis on Hilbert space, whose projections depend on the coset with invariant measure.

value

$$E_N(\beta, \gamma) = \langle g; N, \beta, \gamma | \hat{H} | g; N, \beta, \gamma \rangle \quad (23)$$

that can be calculated with recursive techniques [27, 95, 96]. Thus, one obtains a function of β, γ and the parameters of the hamiltonian, that can be studied as a classical function to find phases, critical points and phase transitions. Often this function can be used as an effective Total Energy Surface (remember that it already contains kinetic terms) or a potential for the collective model can be extracted in some way. This functions can be also useful in other ways: for example, in a γ -independent phase transition, the condition to find the critical point is

$$\frac{d^2 E_N(\beta)}{d\beta^2} = 0, \quad (24)$$

that is easily applied to the above function.

Several useful results on the application of coherent states to the calculation of matrix elements are collected in Refs. [95, 96].

8 QPT in even-even nuclear systems

In this section the Quantum Phase Transitions occurring in algebraic models of even-even nuclear systems will be reviewed, concentrating on the spherical to γ -unstable and on the spherical to axially deformed transitions. These are the most important and the backbones for other transitions that have been studied in the literature.

8.1 Spherical to γ -unstable

This quantum shape phase transition has been the most studied because the transition from the U(5), i.e. spherical phase, to the SO(6), or deformed γ -unstable phase, preserves the sub-chain of symmetries $SO(5) \supset SO(3) \supset SO(2)$ and therefore, a suitable hamiltonian for this phase transition is easy to diagonalize in a basis labeled by the quantum numbers of this chain of subgroups.

In one of the first studies, following Ref. [47] on the full phase transition, namely Ref. [46], it was argued that the true critical point is found when the energy surface takes a pure quartic β^4 function, rather than a square well, as in the first panel of Fig. 4. This equation does not admit an exact solution⁴, but can be solved numerically and the results are not too far from the predictions of the E(5) model, but not too close either. The E(5) remains as a good model, but the analysis of experimental data should better be compared with the results of the quartic potential, in my opinion. For instance, the ratio $R_{4+ / 2+}$ takes the value 2.09, rather than 2.20. This, and other simple indicators, such as ratios of energies and transition rates, are given in the tables of Ref. [46]. Other details can be found in Sect. 3.9.3 of Ref. [36].

The spectrum of the critical point quartic potential is shown in Fig. 14. The degeneracy pattern and quantum numbers are the same as for the E(5) model, but differences arise in the energy ratios and in the position of excited bands (the first excited 0^+ states of the $\xi = 2$ band is lower for instance). Moving now to the corresponding algebraic scheme, one can see that another virtue of the coherent state solution is that it can be computed with growing values of N and this allows to check that, in the large N limit, the IBM hamiltonian at the critical point in the transition from spherical U(5) to deformed γ -unstable SO(6) is represented by the quartic function β^4 . This is another reason why, I believe, too

⁴Technically it is easily diagonalized in the basis of the harmonic oscillator, as the β^4 term, being just the square of β^2 is a monomial in the universal enveloping algebra of U(5), in other words U(5) is still a Spectrum Generating Algebra for this problem.

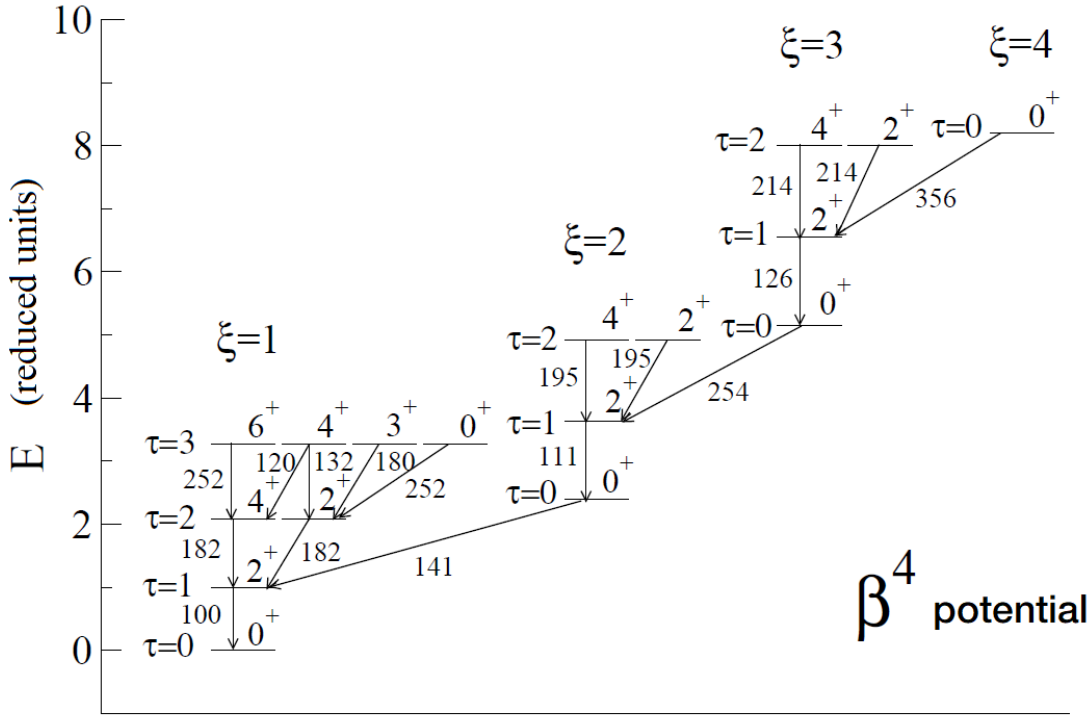


Figure 14: Spectrum of the β^4 potential. Energies can be read from the vertical scale (in reduced units) and arrows indicate B(E2) values normalized to the lowest transition. Courtesy of J.E. García-Ramos and A. Vitturi, adapted.

much an effort has been paid in looking for candidate nuclei that match with the E(5) scheme, while, in reality, the potential at the critical point should be a much smoother β^4 than a square well, with the ensuing differences in the energy scheme. The E(5) is exact, elegant, simple and parameter-free, but it is only somewhat close to what one should expect at the critical point.

Rowe [29] has studied the transition from the vibrational U(5) regime to the γ -unstable rotor, characterized by the SO(6) phase. Here again, the two hamiltonian operators to be mixed have incompatible symmetries, although the level at which the subgroup chains join is just one step away: in fact SO(5) is a common subgroup of both these symmetries and this has the implication that diagonalization is easier than in other cases, because most of the quantum numbers characterizing each irrep are common to both limits. When the mixing parameter is close to the critical value 0.5, the spectrum shows patterns that are remarkably close (though not equal) to the E(5) solution. They become significantly close for a small number of bosons, while for larger values ($N = 20$ and $N = 60$, just to fix ideas) they are closer to the results of the β^4 potential. In Ref. [97, 35] techniques based on the $SU(1,1) \times SO(5)$ basis are exposed and used for diagonalizing numerically the whole shape phase transition from spherical vibrator to γ -soft rotor.

Other hybrid approaches have been proposed [99] that treat the U(5) to O(6) transition and the critical point in ^{134}Ba with different potentials in the Bohr hamiltonian according to the angular momentum (harmonic oscillator for low values of L and square well for larger values) with the idea that the critical point behaviour manifests itself only above a certain threshold, but the improvement appears only marginal at the price of losing the appeal of the simplicity of the E(5) description.

8.2 Spherical to axially deformed

The quantum shape phase transition from spherical to axially deformed shapes (large N limit) corresponds to the transition from the $U(5)$ to the $SU(3)$ limit of the IBM (where N is finite). Rosensteel and Rowe [45] have studied the whole transition using the linear mixing hamiltonian of Eq. (2), because the spherical and axial limits pertain to incompatible symmetries. The diagonalization has been performed in an $SU(3)$ basis that allows for numerical simplifications [100]. The spectrum and several other quantities, such as the $B(E2)$ values and the square of amplitudes are studied in detail. The results show persistence of the limiting symmetries (quasi-dynamical symmetries) down to a narrow region around the critical point, where the spectrum shows approximately the $X(5)$ symmetry up to a scale factor that depends on the number of bosons. This region of strong mixing narrows down to a zero-measure set when the number of particles is increased, thus enlarging the regions of quasi-dynamical symmetries. The $X(5)$ model (let us remind that is derived in the Bohr-Mottelson model) is found to work well in reproducing most of the salient features of the spectrum obtained with the IBM at the critical point, but there are also some noticeable differences, such as interband transitions.

Some properties of a first-order phase transition have been analyzed in Ref. [101], starting from an energy surface, derived from coherent state applied to the IBM-1 with one- and two- body interactions, that contains also cubic terms, i.e.

$$E(\beta, \gamma) = E_0 + N(N - 1) \frac{a\beta^2 - b\beta^3 \cos 3\gamma + c\beta^4}{(1 + \beta^2)^2} \quad (25)$$

where the coefficient expresses the scaling with the number of bosons N . This brings in the possibility that there is a barrier between spherical and deformed minima, but these might coexist around the critical point. This is the typical behaviour of a first-order phase transition that can be visualized as in Fig. 15. From top to bottom, only a spherical minimum exists, appearance of a flex (spinodal point), coexistence of two minima, deformed minimum wins until concavity changes in zero (antispinodal point) and then the deformed minimum is the only one. In the region of the parameter space where two coexisting minima occur, these might also take the same value at the bottom of each respective potential pocket, and this is the definition of the critical point for the first order shape phase transition. The potential (25) and the behaviour represented in Fig. 15 are connected with the so-called cusp catastrophe [102, 11].

Let us also mention, although one should probably start a whole new section to deal with this topic, that approaches based on the Bohr hamiltonian with a sextic potential (that has the property of quasi-solvability) have also been used as an effective way to describe the first-order phase transition [103]. The sextic potential allows to have a spherical and a deformed minimum simultaneously and shows shape coexistence.

8.3 Density functional methods

The framework of relativistic energy-density functional has been applied also to axially symmetric problems [104, 105]. The neodymium isotopic chain has been analyzed in detail as well as neighbouring nuclei, with a formalism that incorporates the collective hamiltonian with Inglis-Belyaev moments of inertia and variable mass parameters (see also [37]). The density functional is constrained by imposing a simultaneous adjustment to binding energies, radii, pairing gaps and also quadrupole moments. This last step is necessary to force the system to produce axial or triaxial shapes. The results show that, in this mass region, there is a good reproduction of data that features a sudden change of structure that can be approximated by the $X(5)$ solution. Similar conclusions have been obtained for some even-even Cerium isotopes, where the potential surface has been found to be relatively flat, evidencing a possible critical-point behaviour [106]. This independent confirmation gives further confidence that the critical point schemes, while containing mathematical approximations, do catch the essential physics.

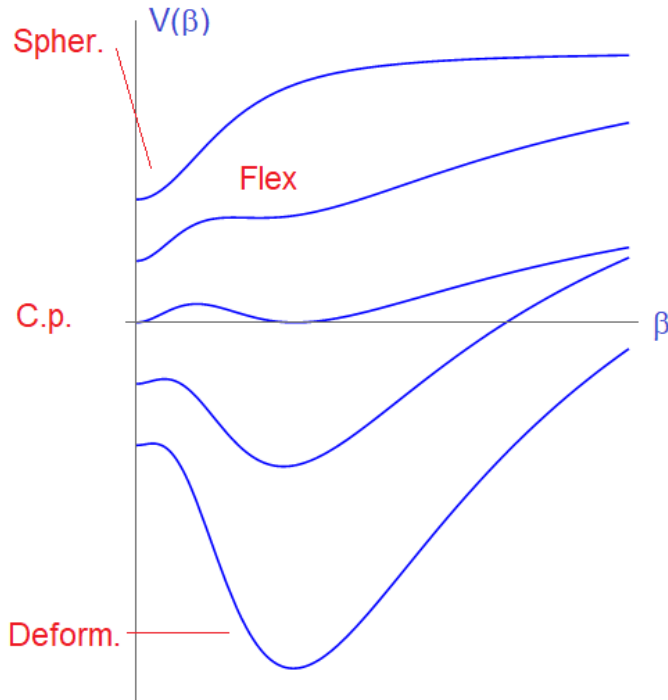


Figure 15: Schematic representations of various potentials of the form (25) with $\gamma = 0$ for simplicity, obtained by varying the parameters. From top to bottom: only a spherical minimum exists, appearance of a flex (spinodal point), coexistence of two minima, deformed minimum wins until concavity changes in zero (antispinodal point) and then the deformed minimum is the only one.

In the sector of odd- A nuclei, recently a study based on a self-consistent relativistic Hartree-Bogoliubov model with deformation constraint has been applied to zirconium isotopes [107]. The even part is treated with the IBM and the unpaired neutron single-particle properties are determined from various constraints. The results indicate that, from light to heavy isotopes in the region $A = 99 - 102$, a transition from triaxial or γ -soft to prolate and then again to triaxial takes place. This is in contrast with previous studies on the same isotopic chain, that did not have the triaxial degree of freedom so well constrained. The isotope ^{99}Zr marks the transitional path with a strong discontinuity.

8.4 Pairing-plus-quadrupole model

Introductory material on pair-coupling models can be found in Refs. [35, 90].

An example of a study on phase transitions in nuclei, that predates the whole story about critical point symmetries, is represented by Ref. [108], where the pairing-plus-quadrupole model (PQM) [109, 110] is used as a schematic model to treat the rotational to superconducting phase transition. This is an example of two incompatible symmetries as in Eq. (2) where the first hamiltonian is the Elliott SU(3) model (some reduced form for a microscopic rotor model hamiltonian) of the type

$$H_1 = -\chi Q \cdot Q \quad (26)$$

where Q is the quadrupole tensor, and the second is Kerman's pairing quasi-spin hamiltonian with constant strength, namely,

$$H_2 = -GS_+S_- \quad (27)$$

that admits analytic solutions through the introduction of an SU(2) spectrum generating algebra. The smallest Lie algebra that contains them both is the symplectic algebra Sp(3). The spectrum can be obtained by diagonalizing the mixed hamiltonian in a basis of $\text{Sp}(3) \supset \text{U}(3) \supset \text{SU}(3) \supset \text{SO}(3)$, in which H_1 is diagonal and H_2 can be constructed as a quadratic function in the elements of Sp(3)⁵. The results of this model show a sharp phase transition between the two phases and a persistence of the rotational structures that survive inside the superconducting phase, that the authors call *superconducting rotor*. This is also linked to the concept of quasi-dynamical symmetry discussed in Sect. 6.1.

8.5 Approaches based on the SU(1,1) affine Lie algebra

Several other investigations have been carried out, using different schemes or different approaches. Useful material and further references can be found in Ref. [35]. For example, one of the most interesting is the introduction of the SU(1,1) affine Lie algebra (quasispin) [111] that allows for an alternative algebrization of a class of hamiltonians of interest to transitional nuclei.

In Ref. [112], the schematic hamiltonian

$$H = (1 - x)\hat{n}_d + \frac{x}{f(N)}\hat{S}^+\hat{S}^- \quad (28)$$

based on the generalized boson pair creation and annihilation operators, $\hat{S}^+ = \frac{1}{2}(d^\dagger \cdot d^\dagger - s^{\dagger 2})$ and $\hat{S}^- = \frac{1}{2}(\tilde{d} \cdot \tilde{d} - s^2)$, is used instead of the consistent-Q hamiltonian. The function $f(N)$ is a linear function of the total number of bosons. The diagonalization of this hamiltonian in a suitable γ -unstable basis allows to extend calculations to a large number of bosons. A dramatic sharpening of order parameters, such as the fractional occupation probability of the d-bosons in the ground state, or the difference between the occupation of the first excited 0^+ and 2^+ states and the g.s., is observed. This enhancement links to quasidynamical symmetries.

Rowe in Ref. [113] gives analytical expressions for algebra elements and matrix elements for the SU(1,1) \times O(N) dynamical group, where the non-compact SU(1,1) algebra acts as a Spectrum Generating Algebra for the “radial” problem, while the additional orthogonal algebra gives the “spherical” or “angular” part, being the basis functions the SO(N)-spherical harmonics on a generalized square-integrable basis. This algebraic scheme is very convenient and very general, the SU(1,1) operators can be represented in terms of raising and lowering oscillator operators (differential operators) and thus an entire class of algebraic problems can be treated with this method: for example, the quartic oscillator or extensions of the Landau potentials become easily tractable in this scheme.

8.6 Triaxiality

Triaxiality arises quite naturally in the collective model, as the condition associated with a potential $V(\beta, \gamma)$ that shows a pocket in the region of non-null β and for $\gamma \neq 0^\circ, 60^\circ$ lying outside of the axial symmetry lines, cfr. Fig. 2.

One can make models for rigid [114] or soft triaxiality [77] by employing potential wells of varying stiffness and study the spectrum and other observables with the Bohr hamiltonian. Not quite so easy is the study of triaxiality in the IBM, where the algebraic structure of the model leads to dynamical symmetries that, up to two-body interactions, imply no triaxial minima, if one uses the coherent state approach to evaluate the corresponding potential energy surface. One needs to go beyond second order and introduce three-body terms to study the triaxial phase [115, 116, 117, 118], or to go to special limits of the proton-neutron IBM2 in which the triaxial shape arises as a consequence of different deformation of the proton and neutron ellipsoids. Another way is to include hexadecapole g-bosons.

⁵In other words, it lies in the Universal enveloping algebra of Sp(3).

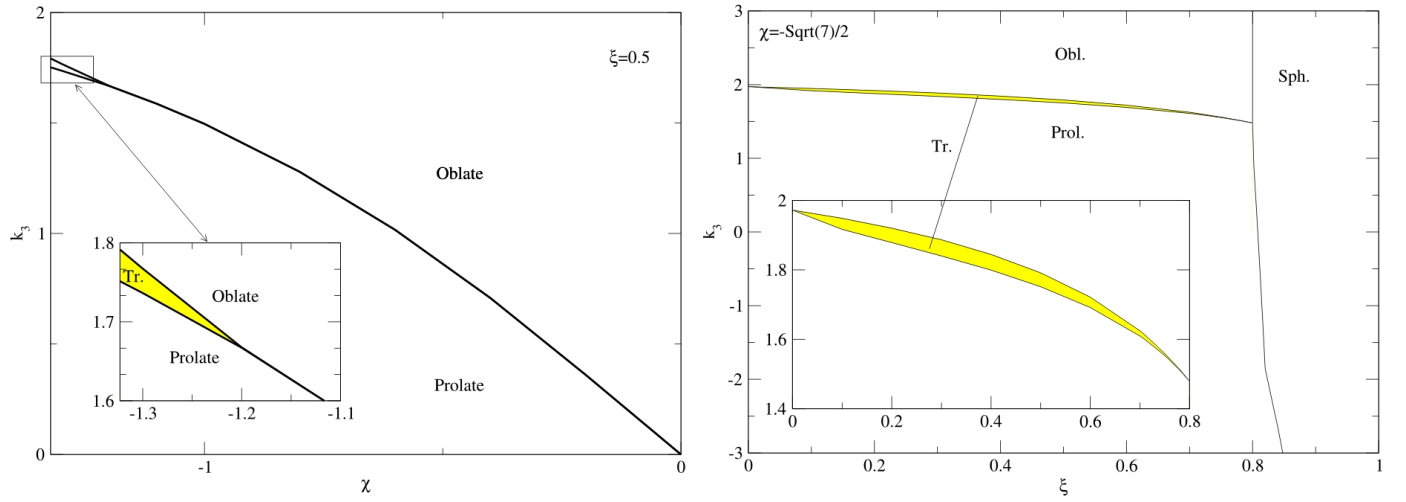


Figure 16: Cuts of the phase diagram of the cubic-Q hamiltonian showing spherical, prolate, oblate and triaxial phases. Adapted from Ref. [118]. The parameters k_3, ξ, χ are those of Eq. (29), where χ , although not written, is contained in the quadrupole operator.

Among the possible additions of cubic terms, the earlier approaches employed various combinations of $[d^\dagger d^\dagger d^\dagger]^{(L)} \cdot [\tilde{d}\tilde{d}\tilde{d}]^{(L)}$ terms [116, 117], while later studies moved to the cubic quadrupole operator $[Q \times Q \times Q]^{(0)}$ [115, 118, 119]. In Ref. [115], an interesting application to osmium isotopes is found, while in Ref. [118] a study of the phase diagram of the cubic-Q hamiltonian :

$$\hat{H} = \xi \hat{n}_d - (1 - \xi) \left[\frac{(Q \cdot Q)}{N} + k_3 \frac{[Q \times Q \times Q]^{(0)}}{N^2} \right] \quad (29)$$

is carried out. Note that the quadrupole operator also depends on the parameter χ . The large N limit potential energy function can be calculated from Eq. (29) with the coherent states, obtaining a function of $\cos(3\gamma)$ and $\cos(3\gamma)^2$. This quadratic expression in $\cos(3\gamma)$ admits axial minima, but also non-axial minima. A complete analysis of the potential energy function shows the presence of a narrow region of the parameter space where a triaxial phase exists, as seen in Fig. 16.

In examining the dynamics of triaxial deformation and the oblate-prolate shape coexistence with use of a (1+3)D collective model in which the β degree of freedom is frozen and one concentrates on the γ degree of freedom (thus disregarding spherical shapes or the typical critical point flat behaviour of the E(5) and X(5) models), Ref. [120] suggests that the excitation energies of 0^+ states can be used as a marker for distinguishing γ -unstable from axially symmetric or rigid triaxial deformation. In particular, electric quadrupole transitions are related to the onset of the oblate-prolate coexistence.

8.7 Pair-transfer

As an additional way to address the evolution of shapes and the phase transitions, the transfer of pairs of correlated nucleons can be studied along a chain of isotopes in algebraic models with the pair-addition, P_+ , and pair-removal operators, P_- , considering a certain set of single-particle states labeled by their total angular momentum j :

$$P_+ = \sum_j [a_j^\dagger a_j^\dagger]_0^{(0)} \quad (30)$$

where the removal operator is obtained by interchanging $a^\dagger \rightarrow a$. The P_+ (P_-) operator connects the ground state of a nucleus with N bosons (or $2N$ nucleons) with all 0^+ states of a nucleus with $N + 1$

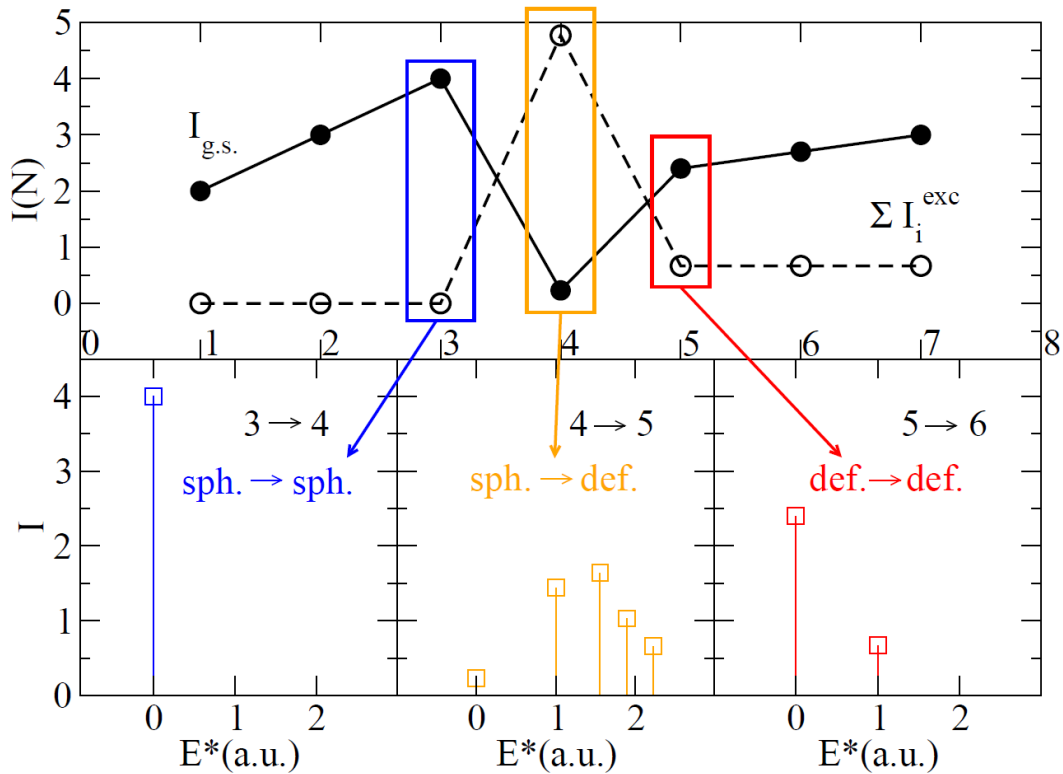


Figure 17: Pair addition intensities from the ground state in the system with N bosons to the ground and excited states (full and empty circles) in the $N + 1$ system as a function of the (arbitrarily chosen) boson number. The system is spherical until $N = 4$, then it has a quick transition to deformed (from $N = 5$ on). The lower panels show the full pair response as a function of energy in arbitrary units in three specific cases: within the spherical phase, across the phase transition (displaying fragmentation) and within the deformed phase.

(or $N - 1$) bosons. The rest of this section will deal with neutron addition and removal only. It is very interesting that the prediction of this model can be tested by measuring pair transfer reactions cross-sections (or ratios thereof). Following Refs. [121, 122], it was shown how these operators can be used to study this by considering a chain of isotopes in the Interacting Boson Model, in which the model hamiltonian performs a transition from $U(5)$ to $SU(3)$ with a sudden jump. Fig. 17 shows the results of calculations in which one assumes that the system is spherical from 1 to 4 bosons and the $SU(3)$ hamiltonian starts to take over at $N = 5$, becoming axially-symmetric afterwards. The intensities (square of matrix elements) of the pair addition, that in this case is simply due to a pair of s^\dagger , are shown. The strength, that is normally found in the ground-state to ground-state transition becomes fragmented into a number of components at the critical point (lower panels). Notice that the white hollow circles in the upper panel here represent the summed intensities to all the excited 0^+ states.

Fig. 18 illustrates the case where two different shape phases coexist in the same system and are associated with the ground state and a given excited 0^+ state. Along a chain of isotopes there might be a mixing of these phases, eventually leading to the interchange of the states, the intruder replacing the ground state from a certain point (critical point). The pair transfer can be again dealt with in the IBM in which the “spherical” phase is obtained through an $U(5)$ hamiltonian with N bosons, associated to the ground state and a second 0^+ “deformed” state is obtained through an $SU(3)$ hamiltonian with $N + 2$ bosons. The microscopic interpretation of the latter is obtained by 2p-2h excitations.

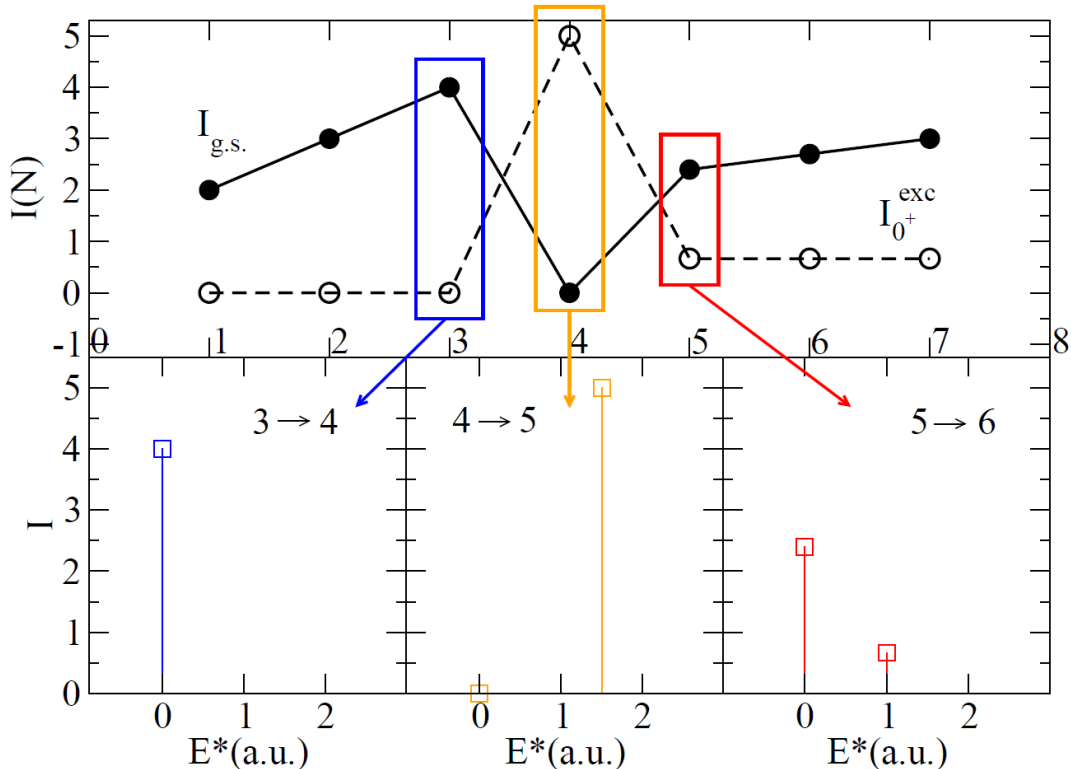


Figure 18: Pair addition intensities to the ground and excited 0^+ states when one has a case of shape coexistence as a function of the boson number (arbitrarily set from 0 to 8). Between $N = 4$ and $N = 5$ a switching occurs between the spherical ground-state configuration and the “intruder” deformed configuration. The full pair response (in arbitrary energy units) is shown for selected cases in the lower frames. No fragmentation occurs. Notice that now the white dots are not anymore representative of the sum of all excited states, but just of a single state.

Because of the difference between the two configurations, the transfer operator is now $s + s^\dagger$, because it can either add a particle-boson or remove a hole-boson (i.e., a correlated pair of fermion holes coupled to zero total angular momentum). Once again, if one assumes that a rapid transition takes place at a certain point (let’s say between $N = 4$ and $N = 5$), one can plot the pair transfer intensities as in Fig. 18. Here, as it can be seen in the second of the lower panels, differently from the previous case, the transfer intensity is almost completely concentrated in a single peak, without the appearance of a fragmentation of strength.

These theoretical calculations must be supplemented with DWBA and CCDC reaction calculations in order to move from intensities (square of matrix elements) to cross-sections, the latter being affected also by kinematic conditions. For example, in collaboration with the Seville and the Tokyo groups we have performed calculations for the (t, p) process on even-even Zr isotopes from $A = 90$ to $A = 100$ using two-particle transition amplitudes coming from Monte Carlo Shell Model calculations. The results show a situation that is similar to the case of shape coexistence described above, if one assumes that, together with the deformed ground state, there is a spherical 0_4^+ excited state. Differential cross-sections are shown in Fig. 19 and the reader is referred to Ref. [122, 123] for further details.

${}^A\text{Zr}(t,p){}^{A+2}\text{Zr}$ @ 30 MeV
cross section at maximum around 40°

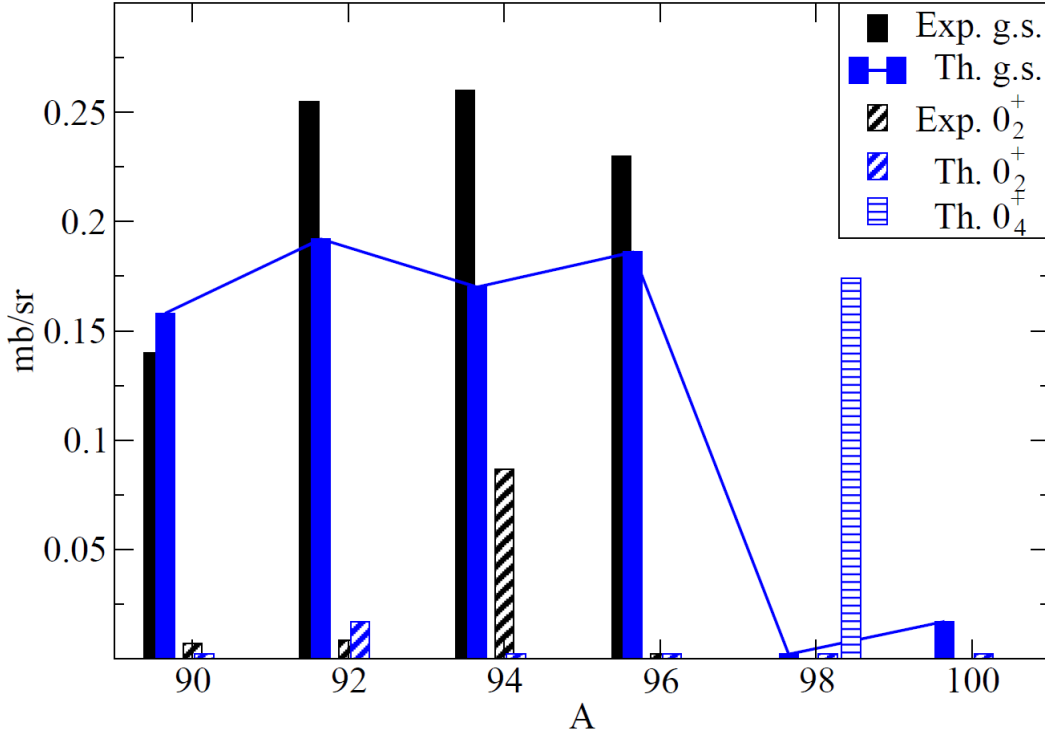


Figure 19: Differential cross sections (at the maximum around 40°) for pair transfer reactions induced by triton beams on the Zirconium chain. Experimental data are taken from [125]. An abrupt switch of the transfer intensities is predicted between $A = 96$ and 98 .

8.8 Mean-field PES mapped to IBM

Nomura and collaborators have proposed [124] to perform Hartree-Fock plus BCS calculations with some versions of the Skyrme functionals to obtain microscopic mean-field potential energy surfaces. These are used as a reference to map or fit a PES obtained within the IBM. The determination of the best parameters in the IBM hamiltonian that reproduce the microscopic theory for the g.s. properties allows to extend the calculations to excited states. Thus spectra and transitions rates can be easily calculated for all the regions where the Skyrme functional has been successfully employed.

9 QPT in odd-even nuclear systems

This section deals with the same topic of the preceding, but for odd-even systems. The reference model is thus the IBFM, rather than the IBM and the odd system is modeled as a bosonic core plus one fermion. This implies that the IBFM cannot be expected to cover all of the possible excitations of the system, i.e., there might be more states at high energies than the one predicted by the model, because at some energy one will start breaking pairs, but one might expect the IBFM to be accurate, taking into account single-particle fermionic degrees of freedom and bosonic core-excitations up to a few MeV's. The connection between bosonic-fermionic models and the underlying geometry is obtained through the intrinsic-frame formalism [94, 126] that allows to obtain several analytic expressions for the matrix elements and to set up a convenient basis for diagonalization of more complex IBFM hamiltonians

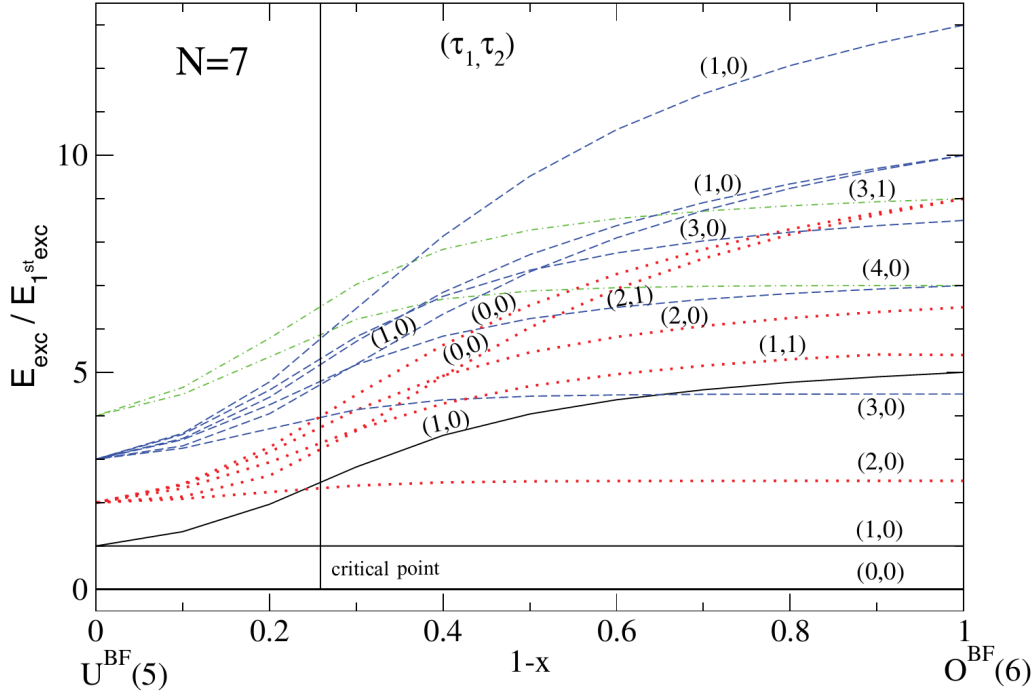


Figure 20: Evolution of the energy spectrum for a number of bosons $N_B = 7$ as a function of the control parameter. States are labeled by the $O^{BF}(5)$ quantum numbers (τ_1, τ_2) along the phase transition. Adapted from Ref. [134].

[127, 128].

Some of the topics of this section have recently been covered in Ref. [129], therefore material will be drawn from that source. Previously, this topic has been reviewed by Petrellis and coauthors [130].

Before delving into this topic, let us also mention that alternative approaches based on the solution of the collective hamiltonian plus a single fermion have also been investigated [131, 132, 133].

9.1 Spherical to γ -unstable in the odd case

As discussed already in the corresponding section for the critical point symmetry $E(5/4)$, i.e., Sect. 6.8.1, the case of $j = 3/2$ is special as it allows to preserve the γ -instability [81, 134] and gives rise to a supersymmetric case. A comparison of the even-even case with an odd-even case for the $j = 3/2$ orbital while the core undergoes a spherical to γ -unstable transition has already been depicted in Fig. 12 and discussed in Sect. 6.11. In Fig. 13 instead, a comparison of evolution of the spectra between the supersymmetric $j = 3/2$ case and the $j = 5/2$ case is shown. Clearly, other values of j can be studied but they do not differ qualitatively from the $j = 5/2$ case.

In Fig. 20 one sees the evolution of energy levels from the harmonic limit to the γ -unstable limit as a function of some (linear, inverted) control parameter. The first excited multiplet is highlighted with black color and splits almost immediately out of the spherical side, as well as all other multiplets. The critical point is indicated by the vertical line. An additional set of quantum numbers that are strictly valid only at the γ -unstable limit can be associated to each line, but the detailed discussion of all of these quantum numbers goes beyond the scopes of the present review paper.

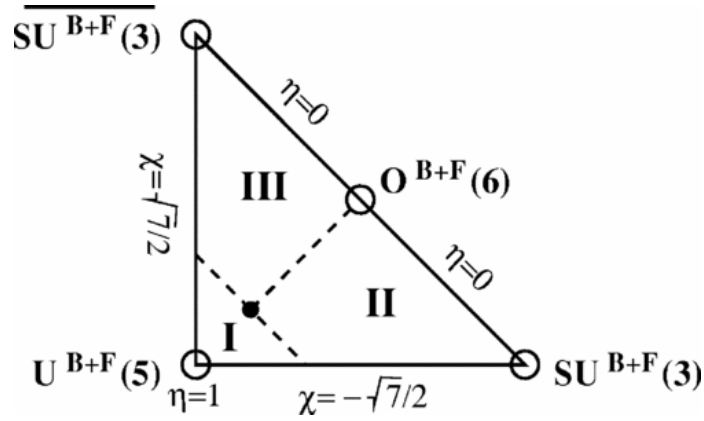


Figure 21: Schematic phase diagram obtained from an extension of the consistent-Q hamiltonian to the odd-A sector. The phases and symmetries here represented extend those of the Casten triangle, with analogous names and meaning, but for the Bosonic-Fermionic system. The triangle is divided into spherical (I) prolate deformed (II) and oblate deformed (III) regions, separated by 1st order phase transitions (dashed lines). The solid dot is the second order phase transition E(5/12). The values of parameters refer to Eq. (31). From Ref. [83]. Courtesy of APS and SciPris.

9.2 Supersymmetry and quantum phase transitions

The idea of supersymmetry (SUSY) and bosonic-fermionic symmetries [135], that makes use of the concept of graded Lie algebras or superalgebras, was introduced in nuclear physics and some evidence has been found that nuclei in the gold-platinum-iridium region do show signs of supersymmetric behaviour [136]. Therefore, it is a natural step to merge these ideas with the shape quantum phase transitions and look for schemes that can match observed patterns in nuclear data. One of the easiest ways to proceed is to extend the consistent-Q formalism to the odd-A sector by coupling the U(6) bosonic algebra of the Interacting Boson Model with the U(12) fermionic unitary algebra arising from the set of $j = \{1/2, 3/2, 5/2\}$ orbitals in which a single nucleon can roam. The model amounts to an U(6/12) superalgebra in which one can write a simple hamiltonian with two terms that compete through a single parameter, η , namely

$$\hat{H} = a \left\{ \eta \hat{C}_1[U^{BF}(5)] - \frac{1-\eta}{N} \hat{Q}_\chi^{BF} \cdot \hat{Q}_\chi^{BF} \right\}, \quad (31)$$

that, aside from an overall multiplicative energy scale a , contains the linear Casimir operators of the five-dimensional unitary algebra (corresponding to the spherical case) and the quadrupole-quadrupole operator (linked to the quadratic Casimir operator of the deformed algebras) [86]. With this hamiltonian, by varying χ and η it is possible to explore a very rich phase diagram, analogous to the Casten triangle, but extended to the odd sector, that is depicted in Fig. 21. See also Sect. 6.10.

Clearly one can study energy spectra, electromagnetic transitions and other observables (see next section) within these schemes.

9.2.1 One-particle transfer

It has been suggested [138] that one-particle spectroscopic intensities might be a good signature for shape-phase transitions in the odd systems along the whole transition from spherical to γ -unstable shapes. Using both the IBM and the IBFM one can calculate matrix elements of the creation operator,

schematically,

$$\langle odd || a_{3/2}^\dagger || even \rangle, \quad (32)$$

where the *odd* state refers to the boson-fermion system and the *even* state to the pure bosonic counterpart. At the extremes of the phase transitions, in the spherical and γ -unstable limits, and especially at the critical point, the calculation can be done analytically. For example, using the exact expressions of the wavefunctions coming from the E(5) and E(5/4) models one can get a selection rule based on orthogonality: only the one-particle addition/removal from ground state to ground state is allowed, all other strengths being zero. The one-particle transfer intensities and the selection rules can be added to the list of important observables that help discriminating between various types of phase transitions.

9.3 Spherical to deformed in the odd case

The phase transition from spherical to stable axially deformed shape is studied in odd nuclei within the Interacting Boson Fermion Model. The extra nucleon can occupy a single j shell or a set of orbitals, the choice $j = \{1/2, 3/2, 5/2\}$ being special.

In Ref. [139], the transition from spherical to oblate shapes is studied with the consistent-Q hamiltonian for the even-even part coupled to a $j = 9/2$ orbital for the single fermion through a quadrupole-quadrupole interaction. Fig. 22 shows the evolution of the energy surfaces for the even-even core (with $N_B = 5$) and for the states of the odd system with different values of K within the orbital with $j = 9/2$. The parameter controlling the shape phase transition is changed from 0 to 1 moving the system from the spherical shape, corresponding to U(5) with a minimum in $\beta = 0$, to the oblate shape, corresponding to $SU(3)$ with a minimum in $\beta < 0$ and passing through the first order critical point (indicated in several panels). The inserts show the typical double-well feature with degenerate minima appearing at the critical point.

Similarly to the previous case, one can diagonalize the hamiltonian for the spherical to deformed shape phase transition with the fermion moving in the set of orbitals $j = \{1/2, 3/2, 5/2\}$ [127]. Now the fermion quadrupole operator will contain a larger number of terms, the coupling term becoming slightly more involved, but the idea is the same. The result of diagonalization for the case of $N_B = 9$ bosons can be seen in Fig. 23, where one can appreciate the different position at which the even and odd critical points appear. The extra fermion does not change qualitatively the picture, but it has the effect of moving (retarding) the phase transition of a little amount (indicated by vertical lines).

Another interesting observation on this system can be done by looking at Fig. 24. It depicts the cuts along $\gamma = 0^\circ$ of the PES for the even system (dashed violet line) and odd system (black lines corresponding to various intrinsic states). The leftmost panel shows the $SU^{BF}(3)$ limit, with deformed minima. The central panel shows the calculations at the critical point of the even system (notice that the violet line is practically flat, with a small bump, invisible in the picture). The rightmost panel shows the critical point of the odd system. One might notice that the line representing the even system in this case still shows a spherical minimum ($\beta = 0$), while the ground state of the system shows the typical first order phase transition PES, with two minima, separated by a barely visible bump.

9.4 Prolate to oblate shape phase transitions in odd nuclei

The prolate to oblate quantum shape phase transition in odd-even nuclei has been recently investigated in Ref. [140] using the coherent states in the interacting boson-fermion model. The bosonic core undergoes a transition from prolate to oblate and it is coupled to a fermion occupying a single orbital. The value $j = 9/2$ was chosen as an example and the effect of the coupling on the odd nucleus has been studied in detail along the transitional path that goes through γ -unstable shapes.

The naive expectation that all the magnetic substates of the odd nucleus would be driven by the bosonic core are, in fact, not realized and several interesting observations can be made: two out of the

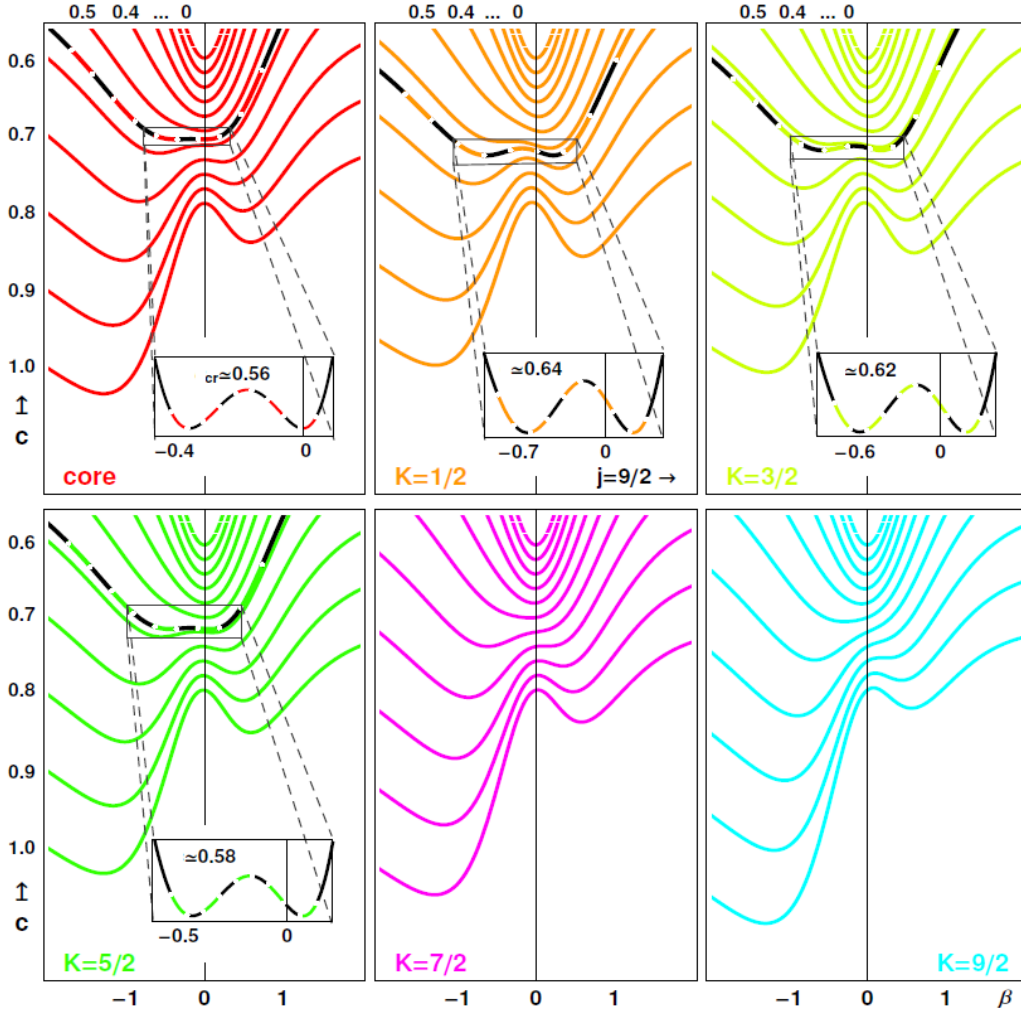


Figure 22: Energy surfaces for the even core (with $N_B = 5$) and for the states of the odd system with different values of K with $j = 9/2$. The parameter controlling the shape phase transition is changed from 0 to 1 moving the system from the spherical shape, corresponding to $U(5)$, to the oblate shape, corresponding to $SU(3)$ and passing through the critical point (indicated in several panels).

five K -components of the $j = 9/2$ state slowly evolve from prolate to oblate shapes passing through very γ -soft triaxial shapes. The other three states jump from prolate to oblate shapes and shape coexistence can be found. One of these three states shows a very pronounced γ -softness.

This rich behaviour is collected in Fig. 25, where one can see the value of γ and the energy at the minimum of the PES, or a fixed β , in panel A). These are shown for the 5 components of the $j = 9/2$ state as a function of the parameter χ . In panel B) the minimum energy is shown as a function of γ for selected values of χ and in panel C) the minima are displayed as dots in the β, γ plane as a function of $\chi \in [-\sqrt{7}/2, \sqrt{7}/2]$.

9.5 Recent experimental and theoretical studies

A number of recent papers have concentrated on experimental evidences of QPT in odd-even nuclei [141, 142, 143, 144, 145, 146, 147, 148]. The spherical to γ -unstable shape phase transition has been

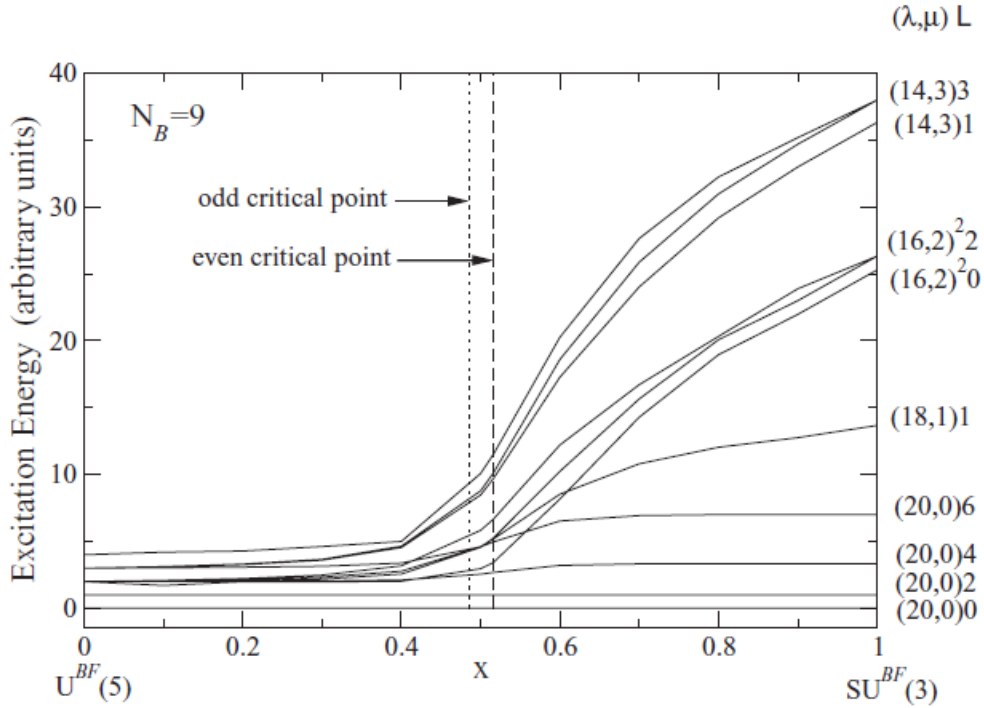


Figure 23: Normalized energy levels of the odd-even system with nine bosons along the spherical to deformed shape phase transition. States are labeled with by the asymptotic SU(3) quantum numbers (λ, μ) and the angular momentum.

studied for the odd nuclei $^{127-137}\text{Ba}$, $^{101-109}\text{Rh}$ in Ref. [141], for the $^{103-109}\text{Rh}$ nuclei also in Ref. [146] and for $^{123-135}\text{Xe}$ nuclei [142] using the IBFM. Again $^{129-137}\text{Ba}$, $^{127-135}\text{Xe}$, $^{129-137}\text{La}$ and $^{127-135}\text{Cs}$ are studied in Ref. [144, 145] considering that the respective bosonic cores, i.e., $^{128-136}\text{Ba}$ and $^{126-134}\text{Xe}$ show a spherical to γ -soft phase transition.

The spherical to axially-deformed quantum shape phase transition is studied in Ref. [143] for the $^{147-155}\text{Eu}$ and $^{147-155}\text{Sm}$ isotopes. The odd-mass europium isotopes, $^{149-155}\text{Eu}$, are also analysed in Ref. [147]. Finally, the transition from prolate to oblate shapes passing through the γ -unstable or the triaxial regions has been investigated for the $^{185-199}\text{Pt}$, $^{185-193}\text{Os}$ and $^{185-195}\text{Ir}$ isotopes using the IBFM plus self-consistent Hartree-Fock-Bogoliubov calculations [148].

10 Models with two-fluids

10.1 Two-fluids in algebraic models

Quantum phase transitions have been studied also in two-fluid models, such as the IBM-2, that distinguishes between the proton and the neutron bosons [150, 151]. These are then treated as in the IBM, with the approximation of scalar and quadrupole pairs, that are the building blocks of two U(6) symmetries. The total underlying algebra is thus $U(6) \times U(6)$ that, among the many possibilities, supports four basic dynamical symmetries, that can be associated to those of the IBM-1 in a straightforward manner. The IBM hamiltonian can be generalized to the IBM-2 case and the quadrupole interaction now displays three terms, a proton-proton, a neutron-neutron and a proton-neutron interaction. The reader might find it useful to check Refs. [135] and [149] to learn more about mixed-symmetry states,

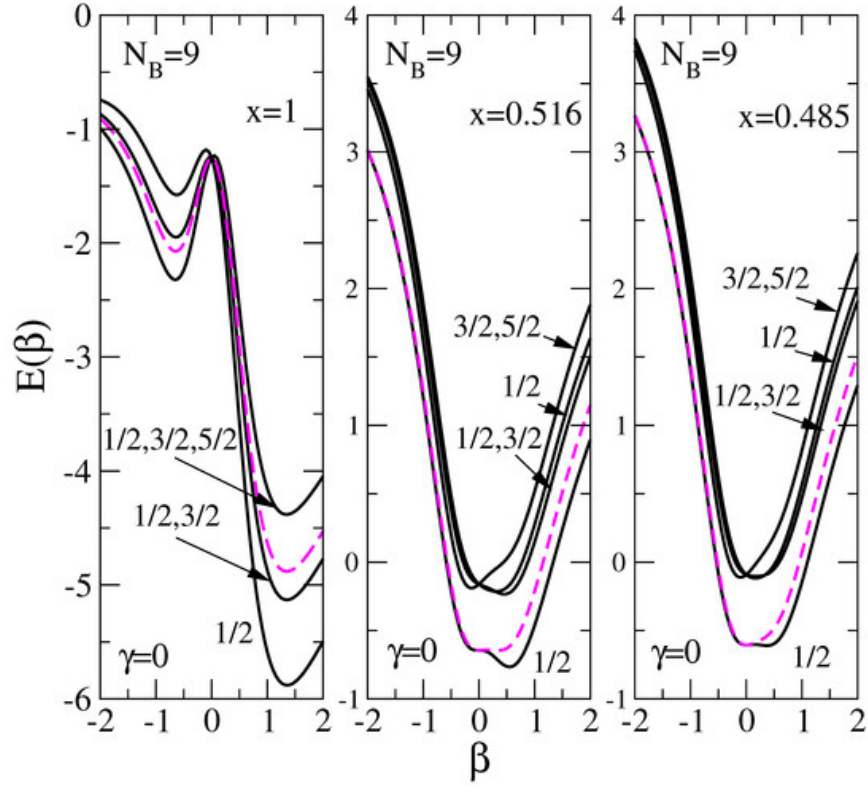


Figure 24: Cuts of the potential energy surfaces at $\gamma = 0^\circ$ for the odd system with $N_B = 9$ as a function of the deformation parameter in three different cases: deformed (left), critical point for the even system (center) and for the odd (right). Several intrinsic states are shown, the dashed lines represent the energy surfaces for the even case.

F-spin and M1 transitions. For example, the consistent-Q IBM-2 hamiltonian takes now the form:

$$x(\hat{n}_{d_\pi} + \hat{n}_{d_\nu}) - \frac{1-x}{N} Q \cdot Q \quad (33)$$

where \hat{n} is the d-boson number operator for protons or neutron and $Q = Q_\pi(\chi_\pi) + Q_\nu(\chi_\nu)$ is the generalized quadrupole operator, sum of the contributions of each fluid.

A major difference arises in this model, namely, the ability to yield triaxial shapes. The axial-triaxial phase transition is found to be of second-order. By defining suitable intrinsic states with the operators in Eq. (22), but with an F-spin index, one can obtain analytic potential energy surface formulas that depend now on $\beta_\pi, \beta_\nu, \gamma_\pi$ and γ_ν plus several more parameters than in the corresponding IBM-1 case. This function has been studied in detail in Refs. [150, 152] and the schematic three-dimensional phase diagram obtained is shown in Fig. 26.

This diagram extends the IBM-1 phase diagram drawn on the Casten's triangle (U(5)-SO(3)-O(6)), that here is found at the bottom basis and includes two new exceptional points, x^* and y , that mark the transition from spherical to triaxial and from axial to triaxial.

The IBM-2 has been also applied to the U(5) to SO(6) transition, in particular a detailed comparison of experimental data in the Palladium region [153] has allowed to identify mixed-symmetry states.

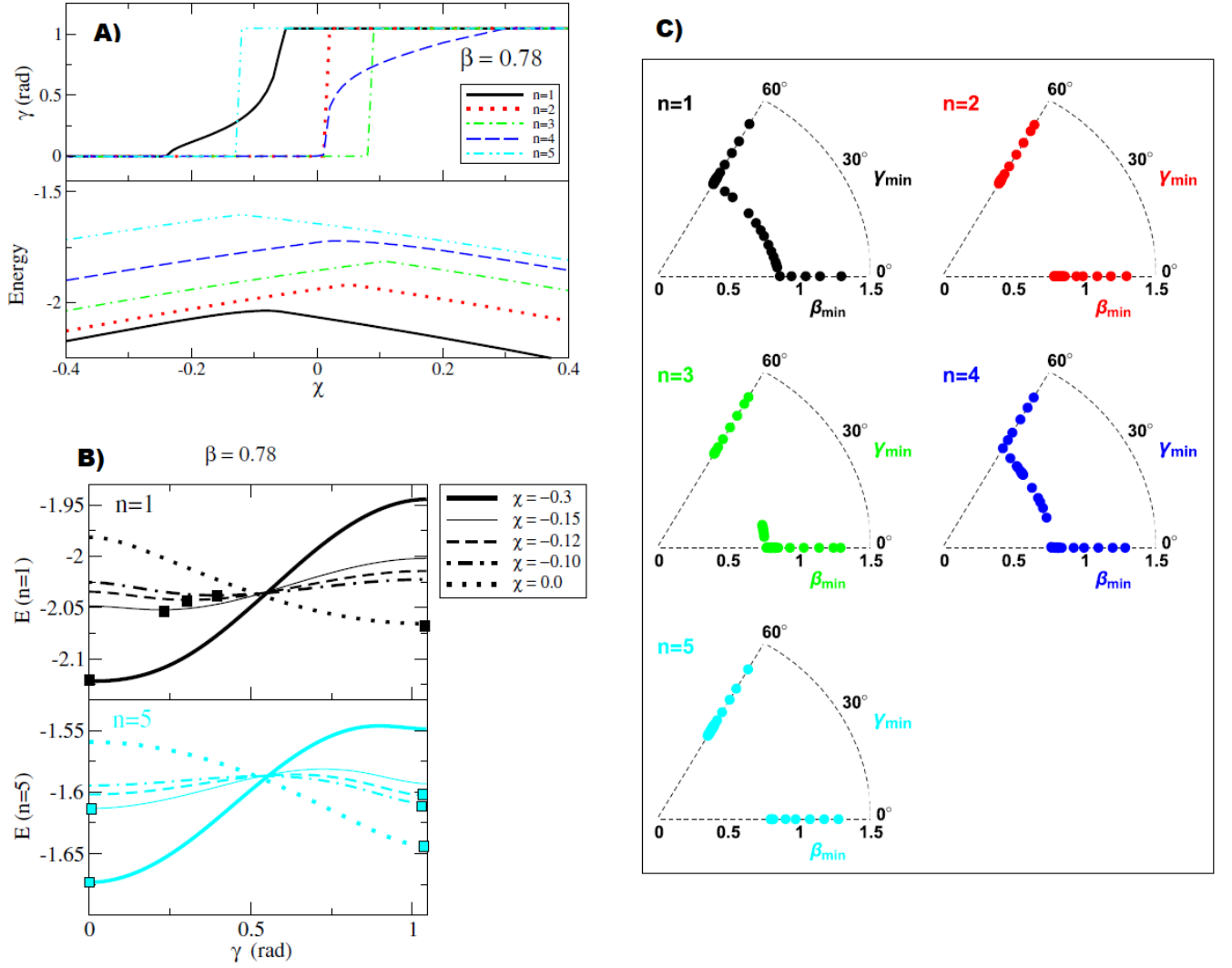


Figure 25: A) For a fixed β , the value of γ and the energy at the minimum of the PES are shown for the 5 components of the $j = 9/2$ state as a function of the parameter χ . B) Minimum energy as a function of γ for selected values of χ . Squares indicate the position of the minimum. C) Minima in the β, γ plane as a function of $\chi \in [-\sqrt{7}/2, \sqrt{7}/2]$. Color codes match throughout the various panels, adapted from Ref. [140].

10.2 Two-fluids in the BM collective model

Models with two-fluids studied in the framework of the Bohr Mottelson collective model have also been tried, although not fully explored yet. In these models one studies the BM quantized motion of two liquid ellipsoidal drops, one for the protons and one for the neutrons, that are coupled by some interaction. The additional degrees of freedom make the model very rich, but it becomes treatable under some simplifying assumptions. For example, in Ref. [154] a simplified model is sketched in which the two ellipsoids have common semi-axes and in which the proton-neutron interaction H_{pn} is proportional to the deformation of each component, namely:

$$H_{pn} = -2G\beta_p\beta_n \sim -G(\langle\beta_p\rangle\beta_n + \beta_p\langle\beta_n\rangle) \quad (34)$$

where the coefficient has been defined in such a way that an approximate separation of variable may hold. Under this approximation, the model becomes solvable and the spectrum depends on the additional

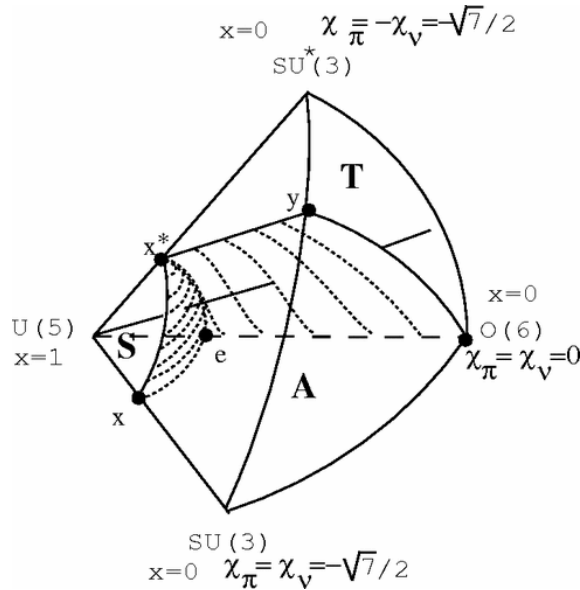


Figure 26: Phase diagram for the IBM-2 model. Four symmetry limits are given at the vertexes with the corresponding defining parameters (see Eq. (33)). Spherical (S), axial (A) and triaxial (T) phases are identified as well as the loci of the corresponding separation surfaces and lines. The phases and critical points of the IBM-1 are found on the triangle at the basis. Courtesy of J.M Arias and J.E. García-Ramos.

parameter G that represents the strength of the proton-neutron interaction.

11 Other models, other domains, other phenomena

Admittedly, this review has concentrated on the surface quadrupole degree of freedom, but there are other degrees of freedom, amenable to a similar collective description, where phase transitions have been discovered and described. For example, the octupole mode is an obvious extension (see next subsection). Another relevant case is the pairing collective model (see Sect. 11.3).

11.1 Octupole

The octupole degree of freedom can also be explored, especially in connection with the quadrupole degree of freedom. It has the additional complication that the underlying space is seven dimensional and the simultaneous description of quadrupole and octupole deformations would require six parameters [159, 160]. This can be simplified for specific octupole deformations, for example, for pear-like axial octupole shapes. Several models for octupole collectivity have been developed that allow to treat quadrupole and octupole degrees of freedom, for instance [161, 162].

Bizzeti has developed a model that works well close to the axial symmetry limit for transitions between the pure harmonic octupole oscillator and permanent asymmetric shapes [163], finding that ²²⁶Th is close to the critical point.

Ref. [164] explores a parameter-free solution (up to an overall scale factor) of the Bohr hamiltonian with quadrupole and octupole degrees of freedom with an L-dependent potential at the critical point between an axial octupole deformation to octupole vibrations, using a square well in the spirit of E(5). The hamiltonian contain also the quadrupole degree of freedom and it belongs to the Analytic

Quadrupole Octupole Axially symmetric models (AQOA). It has been applied to the light actinides, ^{226}Ra and ^{226}Th , where it gives good agreement with data.

11.2 Excited state quantum phase transitions

The phenomenon of quantum phase transitions is not limited to the ground-state, it may occur also in excited states. The study of excited state quantum phase transitions (ESQPT) has shown that several mathematical features arise in the energy spectrum of a system that undergoes some transition: singularities, energy gaps, cusps, etc. Aside from the pure mathematical properties of bosonic and fermionic many-body systems, due to the relative paucity of excited states in nuclei, often these models have been applied to molecular or atomic systems, where the number of excitation phonons is usually much higher (See for instance Refs. [165, 166, 167]). This topic will not be treated in detail in the present review, but the reader is referred to Ref. [10, 168, 9]. Let us just show in Fig. 27 a picture from Ref. [9], where the portion of the spectrum of a consistent-Q hamiltonian, consisting in all the 0^+ states, is shown along the three legs of the Casten's triangle for $N_B = 30$ for a large number of excited states. Here one sees the difference between first- and second- order transitions (first and third panel) that is also demonstrated by the quantity c_1 in the insets that is proportional to the second derivative of the ground-state energy with respect to the parameter η .

The appearance of the phenomenon of excited state quantum phase transitions has been studied also in other schematic algebraic models such as the Lipkin model and two-fluid Lipkin model [169, 11], that are analytically treatable and somewhat simpler, thus allowing a deeper understanding of all the mathematical features that arise in this framework.

11.3 Pairing phase transition

In analogy with the Bohr equation, a pairing collective hamiltonian has been derived by Bès and coauthors [170] :

$$-\frac{\hbar^2}{2B} \frac{\partial^2 \psi}{\partial \alpha^2} - \frac{\hbar^2}{4B} \left(\frac{1}{\mathcal{I}} \frac{\partial \mathcal{I}}{\partial \alpha} - \frac{1}{B} \frac{\partial B}{\partial \alpha} \right) \frac{\partial \psi}{\partial \alpha} + \left(V(\alpha) + \frac{\hbar^2 M^2}{2\mathcal{I}} - E \right) \psi = 0 \quad (35)$$

where α is the deformation of the pair field, in analogy with β of the collective model, B is a mass parameter, \mathcal{I} is a inertial parameter and $M = A - A_0$ is the number of particles relative to a given reference. Depending on the shape of the potential (i.e., the position and structure of its minima), this hamiltonian can be used to describe the transition from normal to superfluid phases [171, 172, 173, 52]. The variable α is a sort of deformation in a fictitious space called the pairing gauge-space.

In Fig. 28, one can see the sequence of energy levels as a function of M (lines are drawn just to guide the eyes) for the three cases of a pairing vibrator (linear), associated with the $U(2)$ algebra, a pairing rotor (quadratic), associated with an $SO(3)$ algebra and the critical point, that has been called $E(2)$ because it is the square well solution that approximates the behaviour between these two algebras, $U(2) \leftrightarrow SO(3)$. The picture also shows the corresponding shape of potentials $V(\alpha)$, see Eq. (35), that possess a ‘‘spherical’’ minimum for the vibrator, a ‘‘deformed’’ minimum for the rotor and a flat behaviour at critical point. These studies demonstrate, for example, that the typical textbook example (Bohr-Mottelson) of pairing vibrations around the closed-shell nucleus ^{208}Pb , lies in fact much closer to the critical point than to the spherical limit. The anharmonicity in the pairing spectrum is, in fact, quite large, a problem that has been around for several years.

Another interesting model for a many-fermion system exhibiting a phase transition from a superconducting to rotational phase has been devised in Ref. [175], where two incompatible symmetries, a microscopic model symplectic hamiltonian for rotational states using a Q-dependent potential and a quadratic fermionic pairing hamiltonian of Racah leading to an $SU(2)$ quasispin algebra, are mixed with

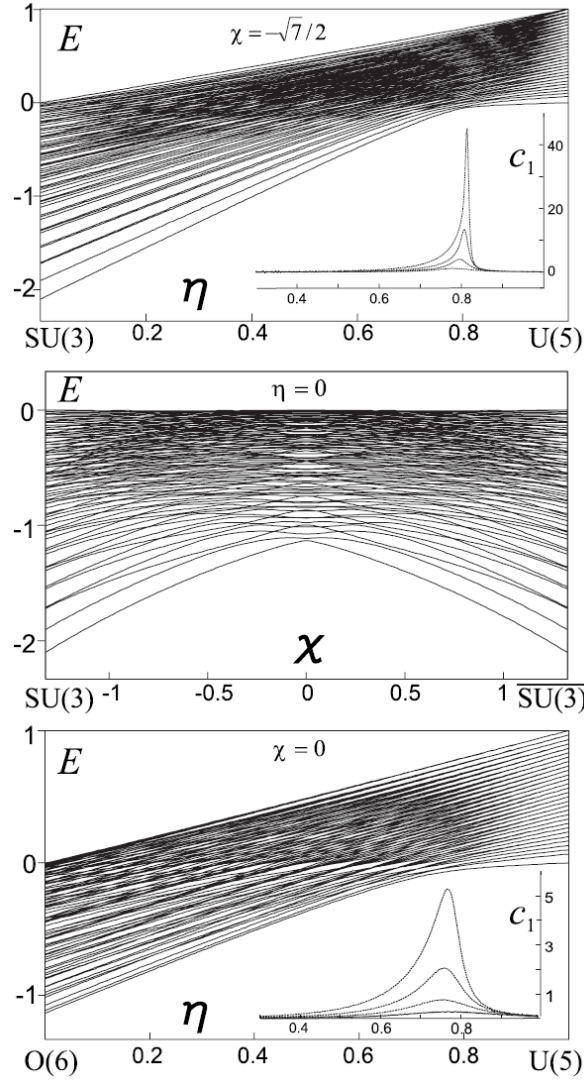


Figure 27: Spectrum of the consistent-Q hamiltonian $\eta \hat{n}_d + \frac{1-\eta}{N_B} \hat{Q}_\chi \cdot \hat{Q}_\chi$ with $N_B = 30$ as a function of the control parameters for the prolate-spherical, prolate-oblate spherical- γ -soft transitions. See text and Ref. [9] for further details. Courtesy of the APS and SciPris.

a linear parametrization. The interesting pioneering model essentially predates many of the subsequent researches in the field and offers insight on the nature of this phase transition.

12 Conclusions

In this review paper, I have tried to summarize the field of quantum shape phase transitions in nuclei and to highlight the differences between algebraic models and collective approaches. I did not make a systematic pedagogical introduction as this has already been covered several times, but I have concentrated on concepts, results and comparisons between the two main models from a slightly off-the-beaten path point of view, hoping that this would bring additional attention to several issues that are still worthy of further investigation.

Aside from the obvious conclusions that the concept of critical point symmetry captures an important aspect of phase transitions and it has stimulated a number of detailed works that have advanced our

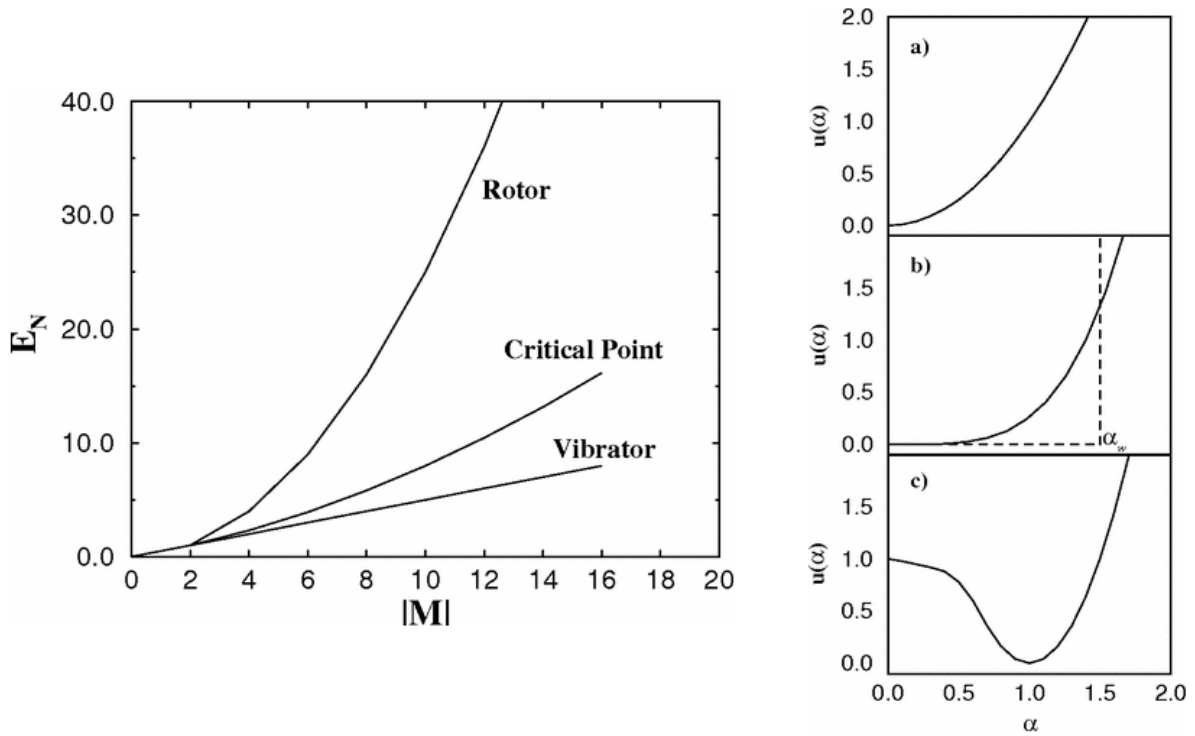


Figure 28: Sequence of energy levels for the three cases of a pairing vibrator, pairing rotor and the E(2) critical point and corresponding shape of potentials $V(\alpha)$, see Eq. (35). The potentials are indicated here in a reduced form, $u(\alpha)$, rather than in the form $V(\alpha)$, but this is irrelevant here. The E(2) solution corresponds to using the square well (dashed line) in place of the quartic potential in the central panel. Figures joined from Ref. [52].

knowledge of spectroscopy, the main conclusion is that theory has gone far beyond experiments in the sector of odd-even nuclei. Not so in the sector of even-even nuclei, where spectroscopy has proceeded at a similar pace with respect to the theoretical models, in a profitable mutual exchange of ideas. Experimentalists in nuclear physics have traditionally found it harder to address problems in odd nuclei, for a number of good reasons (denser spectra, shorter lifetimes, difficulty of interpretation of observed multiplets and so on). The same to a large extent is true for theorists, it is, in fact, much easier to treat bosonic degrees of freedom than fermionic or mixed ones, but in the case of the IBFM and in the case of symmetries of one fermion added to a collective core, the advances have been tremendous, from E(5/4) and E(5/12) to the analysis of all the shape-phase transitional paths discussed in Sect. 9. Except for the work of Fetea et al. [84], a long road has been drawn theoretically, but not yet fully explored from the experimental side and, as it always happens, any deviation from the expected route will be a signal of new discoveries.

I believe, though, that refining the models just for the sake of getting a step closer to what many call “a better reproduction of the data”, has often led researchers astray into too narrow a way, that has departed from the main aim, i.e., understand phenomena. Adding parameters to potentials, without the connection to physics, might be fun or interesting at most, but must be stimulated by experimental ideas and must lead to solid predictions. Very often pages of complex approaches have been published leading to models that work only for this or that isotope and not in general. It is my opinion that this route leads nowhere and that true advance, in the form of solid statements, corroborated by experimental evidences, should rather be searched. The application of symmetries to physical equations or the identification of

patterns in bunches of data are certainly examples of this more virtuous conduct.

Acknowledgements

I wish to thank A. Vitturi, C.E. Alonso and J.M. Arias for our long-standing collaboration on the topics of this review paper and I'd like to thank M. Büyükkata for having recently taken care of Ref. [129] and for the preparation of several figures for our works, that have been included in the present article. I also thank Gagandeep Singh for helping with the task of proofreading.

I acknowledge the APS for the reuse license for Figs. 21 and 27.

References

- [1] L.D. Carr, *Understanding Quantum Phase Transitions*, CRC Press, Taylor and Francis (2011)
- [2] S. Sachdev, *Quantum Phase Transitions, 2nd edition*, Cambridge University Press (2011)
- [3] R.F. Casten, *Nuclear Structure from a simple perspective*, Oxford University Press (1990)
- [4] A. Frank, J. Jolie and P. Van Isacker, *Symmetries in Atomic Nuclei*, Springer Tracts in Modern Physics, Vol. 230 (2009)
- [5] R.F. Casten, P.O. Lipas, D.D. Warner, T. Otsuka, K. Heyde, J. Draayer, *Algebraic approaches to nuclear structure, 1st ed.*, CRC Press (1993)
- [6] R.F. Casten, *Nat. Phys.* 2, 811 (2006)
- [7] R.F. Casten and E.A. McCutchan, *J. Phys. G* 34 (2007) R285
- [8] R.F. Casten, *Phys. Part. Nuclei* 62 (2009) 183-209
- [9] P. Cejnar, J. Jolie, R.F. Casten, *Rev. Mod. Phys.* 82 (2010) 2155
- [10] M.A. Caprio, P. Cejnar, and F. Iachello, *Ann. Phys. (N.Y.)* 323 (2008) 1106
- [11] P. Cejnar, F. Iachello, *J. Phys. A* 40 (2007) 581–595
- [12] G. Jaeger, *Archive for History of Exact Sciences* 53, 51–81 (1998)
- [13] R. Gilmore and D. H. Feng, *Nucl. Phys. A* 301 (1978) 189
- [14] D.H. Feng, R. Gilmore, and S.R. Deans, *Phys. Rev. C* 23 (1981) 1254
- [15] A.E.L. Dieperink, O. Scholten and F. Iachello, *Phys. Rev. Lett.* 44 (1980) 1747
- [16] R. Gilmore, C. M. Bowden, and L. M. Narducci, *Phys. Rev. A* 12 (1975) 1019
- [17] R. Gilmore and D.H. Feng, *Phys. Lett. B* 76 (1978) 26
- [18] J.N. Ginocchio and M.W. Kirson, *Phys. Rev. Lett.* 44 (1980) 1744
- [19] K.-K. Kan, P. C. Lichtner, M. Dworzecka, and J. J. Griffin *Phys. Rev. C* 21 (1980) 1098
- [20] H.J. Lipkin, N. Meshkov and A.J. Glick, *Nucl. Phys. A* 62 (1965) 188
- [21] R. Fossion, C. E. Alonso, J. M. Arias, L. Fortunato, and A. Vitturi, *Phys. Rev. C* 76 (2007) 014316
- [22] A. Frank, P. Van Isacker and C. Vargas *Phys. Rev. C* 69 (2004) 034323
- [23] A. Frank, P. Van Isacker and F. Iachello, *Phys. Rev. C* 73 (2006) 061302(R)
- [24] K. Heyde and J. L. Wood, *Rev. Mod. Phys.* 83 (2011) 1467
- [25] N. Gavrielov, A. Leviatan, F. Iachello *Phys. Rev. C* 99 (2019) 064324
- [26] J.Q. Chen, *Group representation theory for physicists*, World Scientific Publishing Company (1989)
- [27] F. Iachello, *Lie Algebras and Applications*, Lect. Notes in Physics 708 (2006)

- [28] L. Fortunato and W.A. De Graaf, *J. Phys. A* 44 (2011) 145206
- [29] D.J. Rowe, *Nucl. Phys. A* 745 (2004) 47–78
- [30] F. Iachello, *Journal of Physics: Conference Series* 237 (2010) 012014
- [31] J. Jolie, R.F. Casten, P. von Brentano, V. Werner *Phys. Rev. Lett.* 87 (2001) 162501
- [32] E. Santopinto, R. Bijker, F. Iachello *J. Math. Phys.* 37(6) (1996) 2674
- [33] V.K.B. Kota, *Pramana - J Phys* 82 (2014) 743–755
- [34] J. Eisenberg and W. Greiner, *Nuclear Theory, Vol. 1: Nuclear Models- Collective and Single Particle Phenomena*, North-Holland Pub. Co. (1975)
- [35] D.J. Rowe and J.L. Wood, *Fundamentals of Nuclear Models*, World Scientific Publishing Co. Pte. Ltd. (2010)
- [36] L. Fortunato, *Eur. Phys. J. A* 26 (2005) s01
- [37] L. Proćhniak and S.G. Rohoziński, *J. Phys. G* 36 (2009) 123101
- [38] N. Kemmer, D.L. Pursey and S.A. Williams, *J. Math. Phys.* 9, No. 8 (1968) 1224
- [39] S.A. Williams and D.L. Pursey, *J. Math. Phys.* 9, No. 8 (1968) 1230
- [40] E. Chacón, M. Moshinsky and R.T. Sharp, *J. Math. Phys.* 17, No.6 (1976) 668 ,
- [41] E. Chacón and M. Moshinsky, *J. Math. Phys.* 18, No.5 (1977) 870
- [42] L. Wilets and M. Jean, *Phys.Rev.* **102**, 788 (1956)
- [43] P. Baganu and L. Fortunato, *J. Phys. G* 43 (2016) 093003
- [44] D.J. Rowe, *Phys. Rev. Lett.* 93 (2004) 122502
- [45] G. Rosensteel and D.J. Rowe, *Nucl. Phys. A* 759 (2005) 92-128
- [46] J.M. Arias, C.E. Alonso, A. Vitturi, J.E. García-Ramos, J. Dukelsky, A. Frank, *Phys. Rev. C* 68 (2003) 041302
- [47] F. Iachello, *Phys. Rev. Lett.* 85 (2000) 3580
- [48] D. Bés, *Nucl. Phys.* 10 (1959) 373
- [49] J.E. García-Ramos, J. Dukelsky and J.M. Arias, *Phys. Rev. C* 72 (2005) 037301
- [50] E.A. McCutchan and R.F. Casten, *Phys. Rev. C* 74 (2006) 057302
- [51] E.A. McCutchan, N.V. Zamfir and R.F. Casten *Phys. Rev. C* 69 (2004) 024308
- [52] R.M. Clark, M. Cromaz, M.A. Deleplanque, M. Descovich, R.M. Diamond, P. Fallon, I.Y. Lee, A.O. Macchiavelli, H. Mahmud, E. Rodriguez-Vieitez, F.S. Stephens, and D. Ward, *Phys. Rev. C* 69 (2004) 064322
- [53] L. Coquard, N. Pietralla, T. Ahn, G. Rainovski, L. Bettermann, M.P. Carpenter, R.V.F. Janssens, J. Leske, C. J. Lister, O. Möller, W. Rother, V. Werner, and S. Zhu, *Phys. Rev. C* 80 (2009) 061304
- [54] D.G. Ghita, G. Cata-Danil, D. Bucurescu, I. Cata-Danil, M. Ivascu, C. Mihai, G. Suliman, L. Stroe, T. Sava, and N. V. Zamfir *Int. J. Mod. Phys. E* 17 (2008) 1453
- [55] J.M. Arias, *Phys. Rev. C* 63 (2001) 034308
- [56] L. Fortunato, *EuroPhysics News* 40/2 (2009) 25
- [57] R.V. Jolos, *Phys. Part. Nuclei* 35 (2004) 225-250
- [58] R.F. Casten, *Phys. Rev. Lett.* 85 (2000) 3584
- [59] M.A. Caprio, *Phys. Rev. C* 68 (2003) 054303
- [60] A. Frank, C.E. Alonso and J.M. Arias, *Phys. Rev. C* 65 (2001) 014301
- [61] Zhang Jin-Fu, Long Gui-Lu, Sun Yang, Zhu Sheng-Jiang, Liu Feng-Ying, Jia Ying, *Chin. Phys. Lett.* 20 (2003) 1231

- [62] Zhang D.-L., Liu Y.-X. *Chin. Phys. Lett.* 20 (2003) 1028
- [63] M.W. Kirson, *Phys. Rev. C* 70 (2004) 049801
- [64] N. Turkan, *J. Phys. G* 34 (2007) 2235-2247
- [65] F. Iachello, *Phys. Rev. Lett.* 87 (2001) 052502
- [66] M.A. Caprio, *Phys. Rev. C* 72 (2005) 054323
- [67] R. Fossion, *Rev. Mex. Phys.* 54(3), 42 (2008)
- [68] R.F. Casten and N.V. Zamfir, *Phys. Rev. Lett.* 87 (2001) 052502
- [69] R. Bijker, R.F. Casten, N.V. Zamfir and E.A. McCutchan, *Phys. Rev. C* 68 (2003) 064304
- [70] P.G. Bizzeti and A.M. Bizzeti-Sona, *Phys. Rev. C* 66 (2002) 031301
- [71] D. Tonev, A. Dewald et al., *Phys. Rev. C* 69 (2004) 034334
- [72] A. Dewald et al., *Eur. Phys. J. A* 20 (2004) 173
- [73] D. Bonatsos, E.A. McCutchan, R.F. Casten and R.J. Casperson, *Phys. Rev. Lett.* 100 (2008) 142501
- [74] F. Iachello, *Phys. Rev. Lett.* 91 (2003) 132502
- [75] D. Bonatsos, D. Lenis, D. Petrellis and P.A. Terziev, *Phys. Lett. B* 588 (2004) 172
- [76] Yu Zhang, Feng Pan, Yan-An Luo, J.P. Draayer, *Phys. Lett. B* 751 (2015) 423-429
- [77] L. Fortunato, S. De Baerdemacker, and K. Heyde *Phys. Rev. C* 74 (2006) 014310
- [78] R. Fossion, Dennis Bonatsos, and G.A. Lalazissis, *Phys. Rev. C* 73 (2006) 044310
- [79] T. Bayram and S. Akkoyun, *Phys. Scr.* 87 (2013) 6
- [80] F. Iachello, *Phys. Rev. Lett.* 95 (2005) 052503
- [81] B.F. Bayman and L. Silverberg *Nucl. Phys.* 16 (1960) 625
- [82] M.A. Caprio and F. Iachello *Nucl. Phys. A* 781 (2007) 26
- [83] C.E. Alonso, J.M. Arias and A. Vitturi *Phys. Rev. Lett.* 98 (2007) 052501
- [84] M.S. Fetea, R.B. Cakirli, R.F. Casten, D.D. Warner, E.A. McCutchan, D.A. Meyer, A. Heinz, H. Ai, G. Gurdal, J. Qian, R. Winkler, *Phys. Rev. C* 73 (2006) 051301
- [85] D. Bonatsos, Proceedings of the Workshop on Symmetries and Low-Energy Phase Transitions in Nuclear-Structure Physics (Camerino, October 9-11, 2005)
- [86] J. Jolie, S. Heinze, P. Van Isacker and R.F. Casten *Phys. Rev. C* 70 (2004) 011305
- [87] A. Frank, J. Barea and R. Bijker, *Lecture Notes in Physics* 652, 285 (2004)
- [88] M. Moshinsky, *Nucl. Phys. A* 338 (1980) 156-166
- [89] D.J. Rowe, T.A. Welsh and M.A. Caprio, *Phys. Rev. C* 79 (2009) 054304
- [90] D.M. Brink and R.A. Broglia, *Nuclear Superfluidity*, Cambridge University Press (2005)
- [91] D.J. Rowe and G. Thiamova *Nucl. Phys. A* 760 (2005) 59-81
- [92] A.M. Perelomov, *Commun. Math. Phys.* 26, 222-236 (1972)
- [93] J.N. Ginocchio and M.W. Kirson, *Nucl. Phys. A* 350 (1980) 31-60
- [94] A. Leviatan, B. Shao, *Phys. Rev. Lett.* 63 (1989) 2204
- [95] M.A. Caprio, *J. Phys. A* 38 (2005) 6385
- [96] I. Inci, C.E. Alonso, J.M. Arias, L. Fortunato, and A. Vitturi, *Phys. Rev. C* 80 (2009) 034321
- [97] D.J. Rowe, *J. Phys. A* 735 (2004) 372
- [98] P.S. Turner, D.J. Rowe, *Nucl. Phys. A* 756 (2005) 333-355
- [99] A.A. Raduta, A.C. Georghe and A. Faessler, *J. Phys. G* 31 (2005) 337-354

- [100] G. Rosensteel, *Phys. Rev. C* 41 (1990) 730
- [101] A. Leviatan, *Phys. Rev. Lett.* 74 (2006) 051301 ; Erratum-ibid. 74, 059905 (2006)
- [102] T. Poston and I. Stewart, *Catastrophe theory and its applications*, Dover publication, Mineola, New York (1978)
- [103] R. Budaca, P. Baganu, A.I. Budaca, *Phys. Rev. B* 776 (2018) 26 -31
- [104] T. Nikšić, D. Vretenar, G.A. Lalazissis and P. Ring, *Phys. Rev. Lett.* 99 (2007) 092502
- [105] Z.P. Li, T. Nikšić, D. Vretenar, J.Meng, G.A. Lalazissis and P. Ring, *Phys. Rev. C* 79 (2009) 054301
- [106] M. Yu, P.F. Zhang, T.N. Ruan, J.Y. Guo, *Int. J. Mod. Phys. E* 15(4) (2006) 939-950
- [107] K. Nomura, T. Nikšić and D. Vretenar, *Phys. Rev. C* 102 (2020) 034315
- [108] C. Bahri, D.J. Rowe and W. Wijesundera, *Phys. Rev. C* 58 (1998) 1539
- [109] A. Bohr, B.R. Mottelson and D. Pines, *Phys. Rev.* 110 (1958) 936
- [110] S.T. Belyaev, *Mat. Fy. Medd. K.Dan. Vidensk. Selsk.* 31, 11 (1959)
- [111] Feng Pan and J.P. Draayer, *Nucl. Phys. A* 636 (1998) 156
- [112] Feng Pan, Yu Zhang and J.P. Draayer, *J. Phys. G* 31 (2005) 1039
- [113] D.J. Rowe, *J. Phys. A* 38 (2005) 10181
- [114] A.S. Davydov and G.F. Filippov, *Nucl. Phys.* 8 (1958) 237
- [115] P. Van Isacker, *Phys. Rev. Lett.* 83 (1999) 4269
- [116] P. Van Isacker and J.Q. Chen, *Phys. Rev. C* 24 (1981) 684
- [117] K. Heyde, P. Van Isacker, M. Waroquier, and J. Moreau, *Phys. Rev. C* 29 (1984) 1420
- [118] L. Fortunato, C.E. Alonso, J. M. Arias, J.E. García-Ramos, and A. Vitturi, *Phys. Rev. C* 84 (2011) 014326
- [119] G. Thiamova, *Eur. Phys. J. A* 45 (2010) 81-90
- [120] K. Sato, N. Hinohara, T. Nakatsukasa, M. Matsuo and K. Matsuyanagi, *Prog. Theor. Phys.* 123 (2010) 129-155
- [121] C.H. Dasso, H.M. Sofia and A. Vitturi, *Journal of Physics: Conference Series* 580 (2015) 01201
- [122] A. Vitturi, L. Fortunato, I. Inci and J.A. Lay, *JPS Conf. Proc.* 23, 012013 (2018)
- [123] J.A. Lay, A. Vitturi, L. Fortunato, Y. Tsunoda, T. Togashi and T. Otsuka, arXiv:1905.12976v1 [nucl-th]
- [124] K. Nomura, N. Shimizu, T. Otsuka, *Phys. Rev. Lett.* 101 (2008) 142501
- [125] E.R. Flynn, J.G. Beery, and A.G. Blair, *Nucl. Phys. A* 218 (1974) 285
- [126] C.E. Alonso, J.M. Arias, F. Iachello and A. Vitturi, *Nucl. Phys. A* 539 (1992) 59
- [127] C.E. Alonso, J.M. Arias, L. Fortunato and A. Vitturi, *Phys. Rev. C* 79 (2009) 014306
- [128] M. Böyükata, C.E. Alonso, J.M. Arias, L. Fortunato, and A. Vitturi, *Phys. Rev. C* 82 (2010) 014317
- [129] M. Böyükata, C.E. Alonso, J.M. Arias, L. Fortunato and A. Vitturi, *Symmetry* 13 (2021) 215
- [130] D. Petrellis, A. Leviatan, F. Iachello, *Ann. Phys. (N.Y.)* 326 (2011) 926
- [131] Sh. Sharipov and M.J. Ermamatov, *Physics of Atomic Nuclei*, 65, No. 3, 426–436 (2002)
- [132] Sh. Sharipov and M.J. Ermamatov, *Int. J. Mod. Phys. E* 12 (2003) 683–698
- [133] Sh. Sharipov and M.J. Ermamatov and J.K. Bayimbetova, *Physics of Atomic Nuclei* 71, No. 2, 215–220 (2008)
- [134] C.E. Alonso, J.M. Arias, L. Fortunato and A. Vitturi, *Phys. Rev. C* 72 (2005) 061302

- [135] F. Iachello and P. Van Isacker, *The Interacting Boson-Fermion Model*, Cambridge Univ. Press, Cambridge, U.K. (1991)
- [136] A. Metz, Y. Eisermann, A. Gollwitzer, R. Hertenberg, B.D. Valnion, G. Graw and J. Jolie, *Phys. Rev. C* 61 (2000) 064313 ; *ibid. Phys. Rev. C* 67 (2003) 049901
- [137] D. Troltenier, J.A. Maruhn, W. Greiner, V. Velazquez Aguilar, P.O. Hess, and J.H. Hamilton, *Z. Phys. A* 338 (1991) 261-270
- [138] C.E. Alonso, J.M. Arias and A. Vitturi, *Phys. Rev. C* 74 (2006) 027301
- [139] M. Bökükata, C.E. Alonso, J.M. Arias, L. Fortunato and A. Vitturi, *Journal of Physics: Conference Series* 580 (2015) 012047
- [140] M. Bökükata, C.E. Alonso, J.M. Arias, L. Fortunato and A. Vitturi, *Eur. Phys. J. A* 57 (2021) 2
- [141] M.A. Jafarizadeh, M. Ghapanvari, and N. Fouladi, *Phys. Rev. C* 92 (2015) 054306 .
- [142] M.A. Jafarizadeh, N. Fouladi, M. Ghapanvari, and H. Fathi, *Int. J. Mod. Phys. E* 25 (2016) 1650048
- [143] K. Nomura, T. Niksic, and D. Vretenar, *Phys. Rev. C* 94 (2016) 064310
- [144] K. Nomura, T. Niksic, and D. Vretenar, *Phys. Rev. C* 96 (2017) 014304 .
- [145] K. Nomura, R. Rodríguez-Guzmán, and L.M. Robledo, *Phys. Rev. C* 96 (2017) 064316
- [146] M. Ghapanvari, A.H. Ghorashi, Z. Ranjbar, and M.A. Jafarizadeh, *Nucl. Phys. A* 971 (2018) 51
- [147] S. Quan, Z.P. Li, D. Vretenar, and J. Meng, *Phys. Rev. C* 97 (2018) 031301(R)
- [148] K. Nomura, R. Rodríguez-Guzmán, and L.M. Robledo, *Phys. Rev. C* 97 (2018) 064314
- [149] P.O. Lipas, P. von Brentano and A. Gelberg, *Rep. Prog. Phys.* 53 (1990) 1355-1401
- [150] M.A. Caprio and F. Iachello, *Phys. Rev. Lett.* 93 (2004) 242502
- [151] M.A. Caprio and F. Iachello, *Ann. Phys. (N.Y.)* 318 (2005) 454
- [152] J.M. Arias, J.E. García-Ramos, and J. Dukelsky, *Phys. Rev. Lett.* 93 (2004) 212501
- [153] A. Giannatiempo, A. Nannini and P.Sona, *Phys. Rev. C* 58 (1998) 3316
- [154] L. Fortunato, *Nuclear Theory* 24, 280–294 (2005), Proceedings of the XXIV International Workshop on Nuclear Theory, RILA (Bulgaria), Heron press.
- [155] Y. Alhassid and A. Leviatan, *J. Phys. A* 25 (1992) L1265
- [156] A. Leviatan, *Phys. Rev. Lett.* 77 (1996) 818
- [157] P. Van Isacker, *Phys. Rev. Lett.* 83 (1999) 4269
- [158] A. Leviatan and P. Van Isacker, *Phys. Rev. Lett.* 89 (2002) 222501
- [159] P.A. Butler and W. Nazarewicz, *Rev. Mod. Phys.* 68 (1996) 349
- [160] P.A. Butler, *J. Phys. G* 43 (2016) 073002
- [161] N. Minkov, P. Yotov, S. Drenska, W. Scheid, D. Bonatsos, D. Lenis, D. Petrellis, *Phys. Rev. C* 73 (2006) 044315
- [162] N. Minkov, S. Drenska, M. Strecker, W. Scheid, H.Lenske, *Phys. Rev. C* 85 (2012) 034306
- [163] P.G. Bizzeti and A.M. Bizzeti-Sona, *Phys. Rev. C* 70 (2004) 064319
- [164] D. Lenis and Dennis Bonatsos, *Phys. Lett. B* 633 (2006) 474-478
- [165] J. Khalouf-Rivera, F. Pérez-Bernal, M. Carvajal, *J. Quant. Spectrosc. Radiat. Transf.* 261 (2021) 107436
- [166] P. Pérez-Fernández, A. Relaño, J.M. Arias, P. Cejnar, J. Dukelsky, J.E. García-Ramos, *Phys. Rev. E* 83 (201) 046208

- [167] D. Larese, F. Pérez-Bernal, F. Iachello, *J. Mol. Struct.* 1051, 310-327 (2013)
- [168] P. Cejnar, P. Stránský, M. Macek, M. Kloc, *J. Phys. A* 54 (2021) 133001
- [169] J.E. García-Ramos, P. Perez-Fernandez, J.M. Arias, *Phys. Rev. C* 95 (2017) 054326
- [170] D.R. Bès, R.A. Broglia, R.F.J. Perazzo and K. Kumar, *Nucl. Phys. A* 80 (1966) 289
- [171] R.M. Clark, A.O. Macchiavelli, L. Fortunato and R. Krücken, *Phys. Rev. Lett.* 96 (2006) 032501
- [172] R.M. Clark, A.O. Macchiavelli, *Phys. Rev. C* 77 (2008) 057301
- [173] R.M. Clark, *Rev. Mex. Phys. S* 52(4) (2006) 5
- [174] R.M. Clark, A.O. Macchiavelli, L. Fortunato and R. Krücken, *Nucl. Phys. A* 787 (2007) 524c
- [175] D.J. Rowe, C. Bahri and W. Wijesundera, *Phys. Rev. Lett.* 80 (1980) 4394